Theory of thermoreversible gelation and anomalous concentration fluctuations in polyzwitterion solutions *⊗*

Siao-Fong Li; Murugappan Muthukumar **■** ⑩



J. Chem. Phys. 161, 024903 (2024) https://doi.org/10.1063/5.0216981









Theory of thermoreversible gelation and anomalous concentration fluctuations in polyzwitterion solutions

Cite as: J. Chem. Phys. 161, 024903 (2024); doi: 10.1063/5.0216981

Submitted: 2 May 2024 • Accepted: 24 June 2024 •

Published Online: 11 July 2024







Siao-Fong Li¹ and Murugappan Muthukumar^{2,a)}



AFFILIATIONS

- Department of Physics, University of Massachusetts, Amherst, Massachusetts 01003, USA
- ²Department of Polymer Science and Engineering, University of Massachusetts, Amherst, Massachusetts 01003, USA
- a) Author to whom correspondence should be addressed: muthu@umass.edu

ABSTRACT

We present a theoretical framework to investigate thermoreversible phase transitions within polyzwitterion systems, encompassing macrophase separations (MPS) and gelation. In addition, we explore concentration fluctuations near critical points associated with MPS, as well as tricritical and bicritical points at the intersection of MPS and gelation. By utilizing mean-field percolation theory and field theory formalism, we derive the Landau free energy in terms of polyzwitterion concentration with fixed dipole strengths and other experimental variables, such as temperatures and salt concentrations. As the temperature decreases, the dipoles can form cross-links, resulting in polyzwitterion associations. The associations can grow to a gel network and enhance the propensity for MPS, including liquid-liquid, liquid-gel, and gel-gel phase separations. Remarkably, the associations also impact critical behaviors. Using the renormalization group technique, we find that the critical exponents of the polyzwitterion concentration correlation functions significantly deviate from those in the Ising universality class due to the presence of polyzwitterion associations, leading to crossover critical behaviors.

Published under an exclusive license by AIP Publishing. https://doi.org/10.1063/5.0216981

I. INTRODUCTION

The presence of moieties, consisting of permanent electric dipole moment, is ubiquitous in a plethora of both synthetic and biological charged macromolecules. The electrostatic and orientation attributes of such dipolar moieties add a complex layer of additional conceptual challenges to the already existing challenges toward a fundamental understanding of charged macromolecules consisting of only monopolar charges.1 The additional complexity arises from gentle dipole-dipole interactions, compared to the Coulomb interaction among charged units. For example, while the electrostatic interaction energy between two monopole charges separated by a distance r is proportional to 1/r, the interaction energy between two dipoles is proportional to $1/r^3$. Furthermore, if the dipoles are randomly oriented, the interaction energy between two dipoles is proportional to $1/r^6$, and the one between a dipole and a charge is proportional to $1/r^4$. Thus, the presence of dipoles generates a spectrum of spatial range of interactions, which, in turn, is self-consistently modulated by the conformational entropy of the macromolecules containing these dipoles. In general, the dipole-dipole interactions are attractive and can readily form pairs

of dipoles (quadrupoles). Such quadrupoles and multipoles can easily assemble and disassemble. When these nanostructures form, the solution of charged macromolecules is not spatially uniform at all length scales. Due to various possible associations of dipoles, branched aggregates can easily form in solutions, and these electrostatically driven physical associations can lead to gelation. Furthermore, these systems can undergo macrophase separation under suitable experimental conditions, such as lower temperature or lower ionic strength in their solutions.

The inherent nature of dipole-dipole aggregation brings the dipolar polymers into the general class of associating polymers, which is of tremendous current interest.^{2–8} However, the role of electrostatics in associating polymers is not fully explored except for a few isolated situations.9 Toward formulating an adequate theoretical framework for the role of dipoles on the thermodynamic and structural properties of dipole-carrying macromolecules, we consider the extreme case of homo-polyzwitterions where each repeat unit is made of a permanent dipole moment. Apart from the interest in a fundamental understanding of polyzwitterions, these molecules are of great importance in industrial settings.1

The primary goal of the present paper is to formulate a theory of the thermodynamic behavior of polyzwitterion solutions using an adequately simple model that contains the essential elements of dipole–dipole interactions, short-range excluded volume interactions, electrostatic screening due to added salt, and chain conformational entropy. In this model, the dipoles can form cross-links in pairs, and the binding free energy, comprising the binding energy of dipoles and the reduction in entropy of cross-links, determines their extent of reaction. There are immense possible association configurations. The associations involve varying numbers of polyzwitterions, and the associations with the same number of polyzwitterions can also feature differing numbers of cross-links when loops exist within them, as observed in simulations. ^{22–24} Similarly, the possible structures of gels are diverse.

To avoid the complexity, we employ mean-field percolation theory, which assumes that associations lack loops in both the pregel and postgel regimes.^{2,25} Meanwhile, although there are multiple theoretical methods for determining the gel structure^{26,27} or, at the least, the number of cross-links within gels, 6,28,29 we focus only on two common approaches: Stockmayer's treatment, where the gel is tree-like, and Flory's treatment, where gels may contain loops. These treatments allow us to calculate the number of cross-links in associations and gels, thereby determining the chemical potentials associated with forming these associations and the gel network. These treatments allow us to calculate the number of cross-links in associations and gels, thereby determining the free energy associated with forming these associations and the gel network. Our model accounts for short-range van der Waals forces and longrange dipole-dipole and dipole-charge interactions. To simplify the screening effects, due to added salt, on the electrostatic interactions among monomers and ions, we restrict ourselves to the Debye-Hückel (DH) approximation. With these assumptions and simplifications, we derive the Landau free energy of the concentrations of associations and gels using the field theory formalism. When studying the chemical equilibriums of associations and the gel, we derive the weight distributions, as well as the threshold concentration of the gelation.

Furthermore, we predict phase transitions in polyzwitterion solutions utilizing the derived free energy. As the temperature decreases, the liquid-liquid phase separation (LLPS) emerges. However, compared to non-associative polymer solutions, the associative polyzwitterion solutions more easily undergo LLPS due to the dipole-dipole interactions within the polymer-rich phase. Moreover, if the concentration in the polymer-rich phase exceeds a specific threshold, a gel will form, resulting in a liquid-gel phase separation. The interplay between gelation and phase separations goes beyond the simple LLPS. 30,31 Therefore, in this paper, we refer to these phenomena as macrophase separations (MPS) rather than LLPS. With higher concentrations, the solution can transition from a homogeneous solution to a homogeneous gel. Our model additionally predicts that the homogeneous gel can undergo further transitions, such as gel-liquid or gel-gel phase separations, upon further cooling. We demonstrate multiple critical points in the polyzwitterion model due to the cooperation of thermoreversible MPS and gelation, which has been previously studied in neutral associative polymer³² and patchy particle solutions.^{33,34} Furthermore, employing the derived Landau free energy accounting for polyzwitterion concentration fluctuations, we can investigate the critical behavior near the transitions, including gelation and MPS, which exhibit distinctly different critical behaviors. MPS is a thermodynamic phase transition and belongs to the Ising universality class, ³⁵ while gelation represents a geometric phase transition and belongs to the percolation universality class. ³¹ By utilizing the renormalization group (RG) technique, we derive the correlation function beyond the Ornstein–Zernike (OZ) form ^{36,37} and discover crossover critical behaviors in MPS because associations lead to a transition from critical to bicritical points. As for the gelation, with the assumptions of tree-like associations, we present a crossover critical behavior due to the coupling between thermal fluctuations of monomer concentration and geometrical percolation.

The remainder of this paper is structured as follows. We present the microscopic model in Sec. II and derive the free energy under several assumptions in Sec. III. In Sec. IV, we provide the key results on the phase diagrams under the treatments of Stockmayer and Flory, along with the presentation of anomalous critical behaviors. The conclusions are present in Sec. V.

II. MODEL

We consider n_p flexible polyzwitterion chains, each with the uniform number of Kuhn segments N with Kuhn segment length ℓ , dispersed in a solution of volume $\Omega\ell^3$ containing n_0 solvent molecules and fully dissociated monovalent electrolyte with n_c cations and n_a anions. Let \vec{p} be the dipole moment of each of the Kuhn segments. Representing the polyzwitterion chains as continuous curves of contour length $L=N\ell$, the partition function $\mathbb Z$ of the system is given by

$$\mathbb{Z} = \frac{1}{n_p! n_0! n_c! n_a!} \int \prod_{\alpha=1}^{n_p} \mathscr{D} \left\{ \frac{\vec{R}(s_\alpha)}{\ell} \right\} \prod_{c=1}^{n_c} \frac{d\vec{r}_c}{\ell^3} \prod_{a=1}^{n_a} \frac{d\vec{r}_a}{\ell^3} \prod_{o=1}^{n_o} \frac{d\vec{r}_o}{\ell^3} \times \exp \left[-\frac{3}{2\ell^2} \sum_{\alpha=1}^{n_p} \int_0^N ds_\alpha \left(\frac{\partial \vec{R}(s_\alpha)}{\partial s_\alpha} \right)^2 - \frac{U_{\text{elc}}}{k_B T} - \frac{U_{\text{vdw}}}{k_B T} \right], \quad (1)$$

where $\vec{R}(s_{\alpha})$ is the s_{α} th segment position of the α th polyzwitterion, and the symbols \vec{r}_c , \vec{r}_a , and \vec{r}_o denote the position of the α th cation, the α th anion, and the α th solvent molecule, respectively. The integral over $\mathcal{D}\left\{\vec{R}(s_{\alpha})/\ell\right\}$ denotes the path integral over the conformations of the α th chain in accordance with the Edwards Hamiltonian given above. The electrostatic interactions $U_{\rm elc}$ among the dipoles and ions are given by

$$\frac{U_{\text{elc}}}{k_B T} = \frac{1}{2} \sum_{\alpha=1}^{n_p} \sum_{\alpha'=1}^{n_p} \int_0^N ds_\alpha \int_0^N ds_{\alpha'} \frac{\ell_B}{\left|\vec{r}_{\alpha,\alpha'}\right|^3} \\
\times \left[\vec{p} \cdot \vec{p}' - 3 \left(\vec{p} \cdot \frac{\vec{r}_{\alpha,\alpha'}}{\left|\vec{r}_{\alpha,\alpha'}\right|} \right) \left(\vec{p}' \cdot \frac{\vec{r}_{\alpha,\alpha'}}{\left|\vec{r}_{\alpha,\alpha'}\right|} \right) \right] \\
- \sum_{c=1}^{n_c} \sum_{\alpha=1}^{n_p} \int ds_\alpha \left(\vec{p} \cdot \frac{\vec{R}(s_\alpha) - \vec{r}_c}{\left|\vec{R}(s_\alpha) - \vec{r}_c\right|} \right) \left(\frac{\ell_B}{\left|\vec{R}(s_\alpha) - \vec{r}_c\right|^2} \right) \\
+ \sum_{a=1}^{n_a} \sum_{\alpha=1}^{n_p} \int ds_\alpha \left(\vec{p} \cdot \frac{\vec{R}(s_\alpha) - \vec{r}_a}{\left|\vec{R}(s_\alpha) - \vec{r}_a\right|} \right) \left(\frac{\ell_B}{\left|\vec{R}(s_\alpha) - \vec{r}_a\right|^2} \right) \\
+ \frac{1}{2} \sum_{c=1}^{n_c} \sum_{\alpha=1}^{n_a} \frac{\ell_B}{\left|\vec{r}_c - \vec{r}_a\right|}, \tag{2}$$

where ℓ_B is the Bjerrum length $e^2/4\pi\varepsilon_0\varepsilon k_BT$ (where k_B is the Boltzmann constant, T is the temperature, e is the electron charge, ε_0 is the vacuum permittivity, and ε is the relative permittivity). $\vec{p}(\vec{p}')$ denotes the dipole moment of the $s_{\alpha}(s_{\alpha'})$ th segment in the unit of $e \cdot \ell$, and the inter-segment distance vector $\vec{r}_{\alpha,\alpha'}$ is given by

$$\vec{r}_{\alpha\alpha'} \equiv \vec{R}(s_{\alpha}) - \vec{R}(s_{\alpha'}). \tag{3}$$

We assume that the size of ions is extremely tiny such that there is no van der Waals interaction for the electrolyte ions. For the excluded volume interactions among the solvent molecules and segments, we model them as the short-ranged van der Waals interaction $U_{\rm vdw}$ given by

$$\frac{U_{\text{vdw}}}{k_B T} = \frac{w_{oo}}{2} \sum_{o,o'=1}^{n_o} \delta(\vec{r}_o - \vec{r}_{o'})
+ \frac{w_{pp}}{2} \sum_{\alpha,\alpha'=1}^{n_p} \int_0^N ds_\alpha \int_0^N ds_{\alpha'} \, \delta(\vec{R}(s_\alpha) - \vec{R}(s_{\alpha'}))
+ w_{op} \sum_{\alpha=1}^{n_o} \sum_{\alpha=1}^{n_p} \int_0^N ds_\alpha \delta(\vec{r}_o - \vec{R}(s_\alpha)), \tag{4}$$

with w_{oo} , w_{pp} , and w_{po} representing the excluded volume parameters among the solvent molecules, among the segments, and between the segments and solvent molecules, respectively. Because the dynamics of electrolyte ions is much faster than that of polyzwitterions, 1,38 we integrate out the degrees of freedom of small ions and implement the (DH) approximation to get U_{elc} in Eq. (1), yielding

$$\frac{1}{n_c! n_a!} \int \prod_{c=1}^{n_c} \frac{d\vec{r}_c}{\ell^3} \prod_{a=1}^{n_a} \frac{d\vec{r}_a}{\ell^3} \exp\left[-\frac{U_{\text{elc}}}{k_B T}\right]$$

$$= \operatorname{cst.} \times \frac{\Omega^{n_c} \Omega^{n_a}}{n_c! n_a!} \exp\left[\Omega \frac{(\kappa \ell)^3}{12\pi} - \frac{U_{\text{elc}}(\kappa)}{k_B T}\right], \tag{5}$$

where the constant includes the divergence of no physical effect, and the dipole-dipole interaction among segments becomes the modified $U_{\rm elc}(\kappa)$,

$$\frac{U_{\rm elc}(\kappa)}{k_B T} = \frac{1}{2} \sum_{\alpha=1}^{n_p} \sum_{\alpha'=1}^{n_p} \int_0^N ds_\alpha \int_0^N ds_{\alpha'} V_{\rm dd} (\vec{R}(s_\alpha) - \vec{R}(s_{\alpha'})), \quad (6)$$

where V_{dd} is the screened dipole–dipole interaction energy defined

$$V_{\rm dd}(\vec{r}) = \frac{\ell_B e^{-\kappa r}}{r^3} \left[(1 + \kappa r) \vec{p} \cdot \vec{p}' - \left(3 + 3\kappa r + (\kappa r)^2 \right) \left(\vec{p} \cdot \frac{\vec{r}}{r} \right) \left(\vec{p}' \cdot \frac{\vec{r}}{r} \right) \right], \tag{7}$$

and the inverse Debye length κ is given by

$$\kappa^2 = 4\pi \ell_B \frac{\overline{\rho_c} + \overline{\rho_a}}{\rho^3}.$$
 (8)

Here, $\overline{\rho}_c$ and $\overline{\rho}_a$ are the homogenous ion concentrations n_c/Ω and n_a/Ω , respectively. Moreover, because the high temperature drives these dipoles to freely rotate about each other, upon averaging with

respect to the dipole orientations, we approximate the dipole-dipole interaction as U_{Kee} given by 1,12,13

$$\frac{U_{\text{Kee}}}{k_B T} = \frac{1}{2} \sum_{\alpha=1}^{n_p} \sum_{\alpha'=1}^{n_p} \int_0^N ds_\alpha \int_0^N ds_{\alpha'} V_{\text{Kee}} (|\vec{R}(s_\alpha) - \vec{R}(s_{\alpha'})|), \quad (9)$$

$$V_{\text{Kee}}(|\vec{r}|) = -\frac{(\ell_B p)^2}{3} \frac{1 + 2\kappa r + 5/3 (\kappa r)^2 + 2/3 (\kappa r)^3 + 1/6 (\kappa r)^4}{r^6} \times e^{-2\kappa r}, \quad |\vec{r}| > \ell,$$
(10)

where we have assumed that the distance between dipoles is larger than ℓ . In addition, we assume that the whole solution is incompressible. Introducing the local concentration variables $\hat{\phi}_o(\vec{r})$ and $\hat{\phi}(\vec{r})$ for the solvent molecules and polyzwitterion segments, respectively,

$$\hat{\phi}_o(\vec{r}) = \ell^3 \sum_{o=1}^{n_0} \delta(\vec{r} - \vec{r}_o), \tag{11}$$

$$\hat{\phi}(\vec{r}) = \ell^3 \sum_{\alpha=1}^{n_p} \int_0^N ds_\alpha \, \delta(\vec{r} - \vec{R}(s_\alpha)), \tag{12}$$

the incompressibility condition at every position \vec{r} is written as

$$\prod_{\vec{r}} \delta[\hat{\phi}_o(\vec{r}) + \hat{\phi}(\vec{r}) - 1]. \tag{13}$$

Combining Eqs. (5) and (9) with Eq. (1), we obtain the partition

$$\mathbb{Z} = \operatorname{cst.} \times \frac{\Omega^{n_c} \Omega^{n_a}}{n_c! n_a!} \exp\left[\Omega \frac{(\kappa \ell)^3}{12\pi}\right] \int \prod_{\alpha=1}^{n_p} \mathscr{D}\left\{\frac{\vec{R}(s_\alpha)}{\ell}\right\}$$

$$\times \prod_{o=1}^{n_o} \frac{d\vec{r}_o}{\ell^3} \frac{\prod_{\vec{r}} \delta\left[\hat{\phi}_o(\vec{r}) + \hat{\phi}(\vec{r}) - 1\right]}{n_p! n_o!}$$

$$\times \exp\left[-\frac{3}{2\ell^2} \sum_{\alpha=1}^{n_p} \int_0^N ds_\alpha \left(\frac{\partial \vec{R}(s_\alpha)}{\partial s_\alpha}\right)^2 - \frac{U_{\text{vdw}}}{k_B T} - \frac{U_{\text{Kee}}}{k_B T}\right]. \quad (14)$$

If the temperature is high enough, the orientational average of the screened dipole–dipole interaction energy ($V_{\text{Kee}} \sim 1/r^6$) is applicable. Meanwhile, at lower temperatures, the dipole orientations are not random and $V_{\rm dd}$ given by Eq. (7) must be used. For example, if two neighboring dipoles, separated by a distance ℓ , are oriented in an anti-parallel manner $(\uparrow\downarrow)$, the dipole–dipole interaction energy $V_{\rm dd}$ is

$$V_{\rm dd} \bigg|_{r=\ell, (\vec{p}, \vec{p}')=(\uparrow, \downarrow)} = -\frac{\ell_B p^2}{\ell^3} (1 + \kappa \ell) e^{-\kappa \ell}. \tag{15}$$

Starting from this general model for polyzwitterion solutions, we present below a field-theoretic treatment of the phase behavior of polyzwitterion solutions containing added salt, after a discussion of dipolar associations and gelation.

III. FIELD THEORY OF ASSOCIATIVE **POLYZWITTERION SOLUTIONS**

A. Associations in polyzwitterion solutions

As the temperature decreases, the dipole-dipole interaction becomes comparable to the thermal energy, leading to the formation of quadrupoles and other multipoles. The binding energy depends on the relative orientation and distance between two dipoles. We assume that the pairwise dipole bound is antiparallel $(\uparrow\downarrow)$ with a distance ℓ , so the binding energy equals

$$-\frac{\ell_B p^2}{\ell^3} (1 + \kappa \ell) e^{-\kappa \ell} = -\frac{\Theta_p}{T} (1 + \kappa \ell) e^{-\kappa \ell}. \tag{16}$$

We define an effective temperature Θ_p to denote the strength of the anti-parallel quadrupole energy in the absence of salt¹¹ as

$$\frac{\Theta_p}{T} \equiv \frac{\ell_B p^2}{\ell^3}.\tag{17}$$

Therefore, once the solution temperature T decreases to the scale of Θ_p , dipole bindings inevitably form, leading to the association of polyzwitterions. These physical associations of dipoles into quadrupoles, aggregates of quadrupoles, and multipoles can result in branched structures that vary in size and shape. These structures naturally contain different numbers of cross-links (quadrupoles) and may contain closed loops. Modeling such complex architectures is challenging. However, we can simplify the process by applying mean-field percolation theory, 25 assuming the absence of loops. This approximation becomes more accurate as the molecular weight of polyzwitterions increases. 39 By considering tree-like associations involving m polyzwitterions containing m-1 pairwise cross-links for a specific architecture, the Boltzmann factor accounting for conformational entropy is given by

$$\mathbb{P}_{arch} = \exp\left[-(m-1)\frac{f_{\text{bind}}}{k_B T} - \sum_{\alpha=1}^{m} \frac{3}{2\ell^2} \int ds_{\alpha} \left(\frac{\partial \vec{R}^{(m)}}{\partial s_{\alpha}}\right)^2\right] \times \prod_{N=1}^{m-1} \delta_{N_c}, \tag{18}$$

where the symbol f_{bind} denotes the binding free energy,

$$\frac{f_{\text{bind}}}{k_B T} = -\frac{\Theta_p}{T} (1 + \kappa \ell) e^{-\kappa \ell} - \Delta s, \tag{19}$$

with the entropy loss $\Delta s = S_{\text{binding}} - S_{\text{unbinding}}$. The binding free energy f_{bind} primarily depends on quadrupoles. However, we should also consider the impact of cross-links on the hydration between polyzwitterions and solvent molecules, which affects the phase diagrams of aqueous polymer solutions, as shown in previous research. We do not include this effect for simplicity. Here, $\vec{R}^{(m)}(s_{\alpha})$ is the s_{α} th segment position of the α th polyzwitterion in the m-association. The symbol $\prod \delta_{N_c}$ represents the multiplication of Dirac delta functions,

$$\prod_{N_{c}=1}^{m-1} \delta_{N_{c}} = \delta \left(\vec{R}^{(m)}(s_{1}) - \vec{R}^{(m)}(s_{2}) \right) \cdots \times \delta \left(\vec{R}^{(m)}(s_{m-1}) - \vec{R}^{(m)}(s_{m}) \right),$$
(20)

where $\delta(\vec{R}^{(m)}(s_{i-1}) - \vec{R}^{(m)}(s_i))$ specifies the cross-link between the s_{i-1} th segment of the (i-1)th polyzwitterion and the s_i th segment of

the *i*th polyzwitterion. By following Stockmayer's method, we derive the number of architectures for tree-like m-associations A_m as^{2,26}

$$A_m = \frac{N^m (Nm - m)!}{m!(Nm - 2m + 2)!},$$
(21)

and the Boltzmann factor of tree-like m-associations containing a_1 the first architecture, a_2 the second architecture, ..., and a_{A_m} the A_m th architecture is then given by

$$\mathbb{P}_{m} = \frac{\prod_{I_{1}=1}^{a_{1}} \mathbb{P}_{I_{1}} \prod_{I_{2}=1}^{a_{2}} \mathbb{P}_{I_{2}} \cdots \prod_{I_{A_{m}}=1}^{a_{A_{m}}} \mathbb{P}_{I_{A_{m}}}}{a_{1}! a_{2}! \cdots a_{A_{m}}!},$$
(22)

where I_a represents the I_a th association with the ath architecture. Furthermore, employing the multinomial theorem, we simplify the Boltzmann factor as

$$\mathbb{P}_{m} = \frac{\exp\left[-n_{m} \frac{\mu_{m}}{k_{B}T} - \sum_{I=1}^{n_{m}} \sum_{\alpha=1}^{m} \frac{\frac{3}{2\ell^{2}} \int ds_{\alpha} \left(\frac{\partial \vec{R}_{1}^{(m)}}{\partial s_{\alpha}}\right)^{2}\right]}{n_{m}!} \times \left(\frac{\prod_{N_{c}=1}^{m-1} \delta_{N_{c}}^{1st \, Arch.} + \dots + \prod_{N_{c}=1}^{m-1} \delta_{N_{c}}^{A_{m}-th \, Arch.}}{A_{m}}\right)^{n_{m}}, \quad (23)$$

where $\vec{R}_I^{(m)}(s_\alpha)$ represents the s_α th segment position of the α th polyzwitterion in the *I*th *m*-associations, $n_m = a_1 + a_2 + \cdots + a_{A_m}$ and μ_m is the free energy associated with the creation of an *m*-association, defined as

$$\frac{\mu_m}{k_B T} = (m-1) \frac{f_{\text{bind}}}{k_B T} - \ln A_m.$$
 (24)

As a result, we rewrite the partition function given in Eq. (14) as

$$\mathbb{Z} = \operatorname{cst.} \times \frac{\Omega^{n_c} \Omega^{n_a}}{n_c! n_a!} \exp \left[\Omega \frac{(\kappa \ell)^3}{12\pi} \right]$$

$$\times \int \prod_{\alpha=1}^{n_p} \mathscr{D} \left\{ \frac{\vec{R}(s_{\alpha})}{\ell} \right\} \prod_{o=1}^{n_o} \frac{d\vec{r}_o}{\ell^3} \frac{\prod_{\vec{r}} \delta \left[\hat{\phi}_o(\vec{r}) + \hat{\phi}(\vec{r}) - 1 \right]}{n_o!}$$

$$\times \exp \left[-\frac{U_{\text{vdw}}}{k_B T} - \frac{U_{\text{Kee}}}{k_B T} \right] \prod_{w=1}^{\infty} \mathbb{P}_m.$$
(25)

B. Gel phase

Thus far, we have not accounted for the presence of a gel network. The gelation occurs when the polyzwitterion concentration surpasses a certain threshold. Under the assumption of tree-like architectures, the gel network must be tree-like at the gelation point. Moreover, we assume that there is one and only one gel network if it forms. Hence, by defining the free energy of a polyzwitterion joining the gel as the limit of μ_m with $m \to \infty$

$$\frac{\mu_g}{k_B T} = \lim_{m \to \infty} \frac{1}{m} \frac{\mu_m}{k_B T} = \left(\frac{f_{\text{bind}}}{k_B T} - \ln \left(\frac{(N-1)^{N-1}}{(N-2)^{N-2}} \right) - \ln N \right), \quad (26)$$

the Boltzmann factor of the gel network is given by

$$\mathbb{P}_{g} = \exp\left[-m_{g}\frac{\mu_{g}}{k_{B}T} - \sum_{\alpha=1}^{m_{g}} \frac{3}{2\ell^{2}} \int ds_{\alpha} \left(\frac{\partial \vec{R}^{(g)}}{\partial s_{\alpha}}\right)^{2}\right] \times \lim_{m \to \infty} \frac{\prod_{N_{c}=1}^{m-1} \delta_{N_{c}}^{1st Arch.} + \dots + \prod_{N_{c}=1}^{m-1} \delta_{N_{c}}^{A_{m}-th Arch.}}{A_{m}}, \quad (27)$$

where the symbol m_g denotes the number of polyzwitterions in the gel network and $\vec{R}^{(g)}(s_\alpha)$ is the s_α th segment of the α th polyzwitterion in the gel network. As the concentration increases beyond the threshold value, if we continue assuming a tree-like gel network, the treatment is called Stockmayer's treatment. On the contrary, we can allow loop formation within the gel network. The free energy of a polyzwitterion joining the gel becomes

$$\frac{\mu_g}{k_B T} = \frac{\Delta \mu_{\text{loop}}}{k_B T} + \lim_{m \to \infty} \frac{1}{m} \frac{\mu_m}{k_B T},\tag{28}$$

where $\Delta\mu_{\rm loop}$ represents the free energy associated with loop formations. Since the precise architecture of the gel network is unknown, it is difficult to analyze $\Delta\mu_{\rm loop}$ from first principles. In view of this, we use Flory's treatment of "shadow root" to derive $\Delta\mu_{\rm loop}$ and inspect the impact of loops within the gel network on the phase diagram of polyzwitterion solutions. The details of Flory's treatment will be discussed in Sec. III D. As a result, by incorporating associations and gelation, the partition function is given by

$$\mathbb{Z} = \operatorname{cst.} \times \frac{\Omega^{n_c} \Omega^{n_a}}{n_c! n_a!} \exp \left[\Omega \frac{\kappa \ell^3}{12\pi} \right] \times \int \prod_{\alpha=1}^{n_p} \mathscr{D} \left\{ \frac{\vec{R}(s_\alpha)}{\ell} \right\} \prod_{o=1}^{n_o} \frac{d\vec{r}_o}{\ell^3}$$
$$\times \frac{\prod_{\vec{r}} \delta \left[\hat{\phi}_o(\vec{r}) + \hat{\phi}(\vec{r}) - 1 \right]}{n_o!} \exp \left[-\frac{U_{\text{vdw}}}{k_B T} - \frac{U_{\text{Kee}}}{k_B T} \right] \mathbb{P}_g \prod_{m=1}^{\infty} \mathbb{P}_m. \tag{29}$$

C. Field theory formalism

Analogous to the local concentration variables $\hat{\phi}_0(\vec{r})$ and $\hat{\phi}(\vec{r})$, we define the concentration variables $\hat{\phi}_g(\vec{r})$ and $\hat{\phi}_m(\vec{r})$ for gel and m-associations, respectively, as

$$\hat{\phi}_g(\vec{r}) = \ell^3 \sum_{\alpha=1}^{n_g} \int_0^N ds_\alpha \, \delta\left(\vec{r} - \vec{R}^{(g)}(s_\alpha)\right), \tag{30}$$

$$\hat{\phi}_{m}(\vec{r}) = \ell^{3} \sum_{I=1}^{n_{m}} \sum_{\alpha=1}^{m} \int_{0}^{N} ds_{\alpha} \, \delta(\vec{r} - \vec{R}_{I}^{(m)}(s_{\alpha})). \tag{31}$$

Using $\hat{\phi}_m(\vec{r})$ and $\hat{\phi}_g(\vec{r})$ and inserting the identity

$$1 = \int \mathscr{D}\{\phi_o\} \mathscr{D}\{\phi_g\} \prod_{m=1}^{\infty} \mathscr{D}\{\phi_m\} \prod_{\vec{r}} \delta[\phi_o - \hat{\phi}_o] \delta[\phi_g - \hat{\phi}_g]$$

$$\times \prod_{m=1}^{\infty} \delta[\phi_m - \hat{\phi}_m],$$
(32)

the partition function in Eq. (29) is rewritten as

$$\mathbb{Z} = \operatorname{cst.} \times \frac{\Omega^{n_{c}} \Omega^{n_{c}}}{n_{c}! n_{a}!} \exp \left[\frac{\Omega \kappa^{3} \ell^{3}}{12\pi} \right] \\
\times \int \mathscr{D} \left\{ \phi_{o} \right\} \mathscr{D} \left\{ \phi_{g} \right\} \prod_{m=1} \mathscr{D} \left\{ \phi_{m} \right\} \exp \left[-\frac{U_{\text{vdw}}}{k_{B}T} - \frac{U_{\text{Kee}}}{k_{B}T} \right] \\
\times \int \prod_{\alpha=1}^{n_{p}} \mathscr{D} \left\{ \frac{\vec{R}(s_{\alpha})}{\ell} \right\} \prod_{o=1}^{n_{o}} \frac{d\vec{r}_{o}}{\ell^{3}} \frac{\prod_{\vec{r}} \delta \left[\hat{\phi}_{o}(\vec{r}) + \hat{\phi}(\vec{r}) - 1 \right]}{n_{o}!} \\
\times \prod_{\vec{r}} \delta \left[\phi_{o} - \hat{\phi}_{o} \right] \delta \left[\phi_{g} - \hat{\phi}_{g} \right] \prod_{m=1}^{\infty} \delta \left[\phi_{m} - \hat{\phi}_{m} \right] \mathbb{P}_{g} \prod_{m=1}^{\infty} \mathbb{P}_{m}. \quad (33)$$

Upon integrating with respect to \vec{R} and \vec{r}_o , we can fully describe the partition function in terms of the concentrations of the associations and the gel. We initiate these integrations by decomposing the concentration field into its homogeneous and fluctuation components using the Fourier transform (FT),

$$\mathscr{F}\{f\} = \int \frac{d\vec{r}}{\ell^3} f(\vec{r}) \exp\left(-i\vec{q} \cdot \vec{r}\right),\tag{34}$$

where we include the factor ℓ^3 to scale quantities with respect to ℓ . The FT of Dirac delta functions is equal to

$$\mathscr{F}\left\{\prod_{\vec{r}} \delta\left[\phi_i - \hat{\phi}_i\right]\right\} = \delta\left[\frac{\phi_i(\vec{0})}{\Omega} - \overline{\phi}_i\right] \prod_{\vec{a} \neq \vec{0}} \delta\left[\phi_i - \hat{\phi}_i\right], \quad (35)$$

$$\mathscr{F}\left\{\prod_{\vec{r}} \delta[\phi_o + \phi - 1]\right\} = \delta\left[\frac{\phi_o(\vec{0}) + \phi(\vec{0})}{\Omega} - 1\right] \prod_{\vec{a} \neq \vec{0}} \delta[\phi_o + \phi], \quad (36)$$

where $\phi_i(\vec{0})$ represents the Fourier transform at the null momentum $\vec{q} = \vec{0}$, ϕ_i represents the homogenous concentrations of each species, and the \vec{q} dependence of ϕ_i and $\hat{\phi}_i$ is not written down explicitly for $\vec{q} \neq \vec{0}$. It is formidable to integrate out the positions $\vec{R}(s_\alpha)$ and \vec{r}_o straightforwardly in Eq. (33). However, by combining the FT of these concentration fields and the Legendre transformation shown in Appendix A (supplementary material), we approximate the integral as a series expansion of the Landau free energy of concentration fields. The integration with respect to \vec{r}_o approximates to

$$\int \prod_{o=1}^{n_o} \frac{d\vec{r}_o}{\ell^3} \frac{\delta \left[\frac{\phi_o(\vec{0})}{\Omega} - \overline{\phi}_o \right] \prod_{\vec{q} \neq \vec{0}} \delta \left[\phi_o - \hat{\phi}_o \right]}{n_o!} \\
\approx \delta \left[\frac{\phi_o(\vec{0})}{\Omega} - \overline{\phi}_o \right] \frac{\Omega^{n_o}}{n_o!} \mathcal{N}_o \exp \left[-\frac{1}{2!} \int_{\vec{a} \neq \vec{0}} \Gamma_o^{(2)} \phi_o^2 + \cdots \right], \quad (37)$$

with the normalized factor

$$\mathcal{N}_o = \int \mathscr{D} \{\phi_o\} \exp \left[-\frac{1}{2!} \int_{\vec{a} \neq \vec{0}} \Gamma_o^{(2)} \phi_o^2 + \cdots \right]. \tag{38}$$

The symbol $\int_{\vec{q}\neq\vec{0}}$ represents the abbreviation of $\int d\vec{q}/(2\pi)^3\ell^3$. Here, the second-order term is equal to

$$\Gamma_o^2(\vec{q}) = \frac{1}{\overline{\phi}_o},\tag{39}$$

and the higher-order terms $\Gamma_0^{(n)}$, $n \ge 3$, are provided in Appendix A (supplementary material).

When integrating with respect to \vec{R} , we start by re-expressing the differential variables $\mathcal{D}\{\vec{R}(s_{\alpha})\}$ as

$$\prod_{\alpha=1}^{n_p} \mathscr{D}\left\{\frac{\vec{R}(s_\alpha)}{\ell}\right\} = \prod_{\alpha=1}^{m_g} \mathscr{D}\left\{\frac{\vec{R}^{(g)}(s_\alpha)}{\ell}\right\} \times \prod_{m=1}^{\infty} \prod_{I=1}^{n_m} \prod_{\alpha=1}^{m} \mathscr{D}\left\{\frac{\vec{R}_I^{(m)}(s_\alpha)}{\ell}\right\}, \tag{40}$$

yielding the approximations

$$\int \prod_{I=1}^{n_{m}} \prod_{\alpha=1}^{m} \mathscr{D} \left\{ \frac{\vec{R}_{I}^{(m)}(s_{\alpha})}{\ell} \right\} \frac{\delta \left[\frac{\phi_{m}(\vec{0})}{\Omega} - \overline{\phi}_{m} \right] \prod_{\vec{q} \neq \vec{0}} \delta \left[\phi_{m} - \hat{\phi}_{m} \right]}{n_{m}!} \mathbb{P}_{m}$$

$$\approx \delta \left[\frac{\phi_{m}(\vec{0})}{\Omega} - \overline{\phi}_{m} \right] \frac{\Omega^{n_{m}}}{n_{m}!} \mathscr{N}_{m} \exp \left[-\frac{1}{2!} \int_{\vec{q} \neq \vec{0}} \Gamma_{m}^{(2)} \phi_{m}^{2} + \cdots \right], \quad (41)$$

$$\int \prod_{\alpha=1}^{n_g} \mathscr{D} \left\{ \frac{\vec{R}^{(g)}(s_\alpha)}{\ell} \right\} \delta \left[\frac{\phi_g(\vec{0})}{\Omega} - \overline{\phi}_g \right] \prod_{\vec{q} \neq \vec{0}} \delta \left[\phi_g - \hat{\phi}_g \right] \mathbb{P}_g$$

$$\approx \delta \left[\frac{\phi_g(\vec{0})}{\Omega} - \overline{\phi}_g \right] \Omega \mathscr{N}_g \exp \left[-\frac{1}{2!} \int_{\vec{q} \neq \vec{0}} \Gamma_g^{(2)} \phi_g^2 + \cdots \right], \tag{42}$$

with the normalized factors

$$\mathcal{N}_m = \int \mathscr{D} \{\phi_m\} \exp \left[-\frac{1}{2!} \int_{\vec{q}} \Gamma_m^{(2)} \phi_m^2 + \cdots \right], \tag{43}$$

$$\mathcal{N}_g = \int \mathscr{D} \{ \phi_g \} \exp \left[-\frac{1}{2!} \int_{\vec{a}} \Gamma_g^{(2)} \phi_g^2 + \cdots \right]. \tag{44}$$

Here, because the precise architecture of the gel network is unknown, we cannot determine the exact form of $\Gamma_g^{(2)}$. However, we do know that $\Gamma_g^{(2)}$ must be proportional to $1/\overline{\phi}_g$, as there will be no gel concentration fluctuation if the gel does not form. The second-order term $\Gamma_m^{(2)}$ is equal to

$$\Gamma_m^{(2)}(\vec{q}) = \frac{1}{mN\overline{\phi}_m} \left(1 + \frac{R_g^2(m) \, q^2}{3} + \cdots \right),$$
 (45)

where the symbol $R_g(m)$ represents the ensemble-averaged radius of gyration of m-associations, and their fractal dimensions will be discussed in more detail later in this paper. The higher-order terms $\Gamma_m^{(n)}$, $n \geq 3$, are provided in Appendix A (supplementary material). In addition, the FT of U_{vdw} is equal to

$$\mathcal{F}\left\{\frac{U_{\text{vdw}}}{k_B T}\right\} = \Omega \left[\frac{w_{oo}}{2} \left(\frac{\phi_o(\vec{0})}{\Omega}\right)^2 + \frac{w_{pp}}{2} \left(\frac{\phi(\vec{0})}{\Omega}\right)^2 + w_{op} \left(\frac{\phi(\vec{0})}{\Omega}\right) \left(\frac{\phi_o(\vec{0})}{\Omega}\right)\right] + \int_{\vec{0} \neq \vec{0}} \frac{w_{oo}}{2} \phi_o^2 + \frac{w_{pp}}{2} \phi^2 + w_{op} \phi \phi_o. \tag{46}$$

Because the FT of V_{Kee} in Eq. (10) is

$$\mathscr{F}\left\{\text{Eq. }10\right\} = \frac{4\pi}{9} \left(\frac{\ell_B p^2}{\ell^3}\right)^2 \left[g(\kappa \ell) - \frac{h(\kappa \ell)}{2} \left(q\ell\right)^2 + \cdots\right],\tag{47}$$

where the high-order terms are not written down explicitly, and

$$g(\kappa \ell) = (1 + 2\kappa \ell + (\kappa \ell)^2 + (\kappa \ell)^3 / 4)e^{-2\kappa \ell}, \tag{48}$$

$$h(\kappa \ell) = (1 + 25\kappa \ell/24 + 5(\kappa \ell)^2/12 + (\kappa \ell)^3/12)e^{-2\kappa \ell},$$
 (49)

the FT of U_{Kee} is equal to

$$\mathcal{F}\left\{\frac{U_{\text{Kee}}}{k_B T}\right\} = \Omega \left[-\frac{2\pi}{9} \left(\frac{\Theta_p}{T}\right)^2 g(\kappa \ell) \left(\frac{\phi_g(\vec{0}) + \sum\limits_{m=1}^{\infty} \phi_m(\vec{0})}{\Omega}\right)^2\right] \\
+ \frac{1}{2} \int_{\vec{q} \neq \vec{0}} \frac{4\pi}{9} \left(\frac{\Theta_p}{T}\right)^2 \left[-g(\kappa \ell) + \frac{h(\kappa \ell)}{2} q^2 + \cdots\right] \\
\times \left(\phi_g + \sum\limits_{m=1}^{\infty} \phi_m\right)^2.$$
(50)

Consequently, by substituting Eqs. (37)–(42), (46), and (50) into Eq. (33), we derive the partition function as

$$\mathbb{Z} = \operatorname{cst.} \times \exp\left[-m_g \frac{\mu_g}{k_B T} - \sum_{m=1}^{\infty} n_m \left(-\ln mN - 1 + \frac{\mu_m}{k_B T}\right)\right] \overline{\mathbb{Z}} \, \delta \mathbb{Z},$$
(51)

where the constant includes the terms of no physical effect. The mean-field part $\overline{\mathbb{Z}}$ is given by

$$\overline{\mathbb{Z}} = \exp\left(-\frac{\Omega \overline{f}}{k_B T}\right),$$
 (52)

where the mean-field free energy of the polyzwitterion solution is equal to

$$\frac{\overline{f}}{k_B T} = \overline{\rho}_c \ln \overline{\rho}_c + \overline{\rho}_a \ln \overline{\rho}_a - \frac{\kappa^3 \ell^3}{12\pi} + \sum_{m=1}^{\infty} \frac{\overline{\phi}_m}{mN} \ln \overline{\phi}_m + (1 - \overline{\phi}) \ln (1 - \overline{\phi}) + \left[\chi + \frac{2\pi}{9} \left(\frac{\Theta_P}{T} \right)^2 g \right] \overline{\phi} (1 - \overline{\phi}).$$
(53)

Here, the symbol χ denotes the Flory–Huggins mixing parameter $w_{op} - (w_{oo} + w_{pp})/2$. The contribution from concentration fluctuation $\delta \mathbb{Z}$ is

$$\delta \mathbb{Z} = \mathscr{N}_{g} \int_{\vec{q} \neq \vec{0}} \mathscr{D} \left\{ \phi_{g} \right\} \exp \left[-\frac{1}{2!} \int_{\vec{q}} \Gamma_{g}^{(2)} \phi_{g}^{2} + \cdots \right] \prod_{m=1}^{\infty} \mathscr{N}_{m}$$

$$\times \int_{\vec{q} \neq \vec{0}} \mathscr{D} \left\{ \phi_{m} \right\} \exp \left[-\frac{1}{2!} \int_{\vec{q}} \Gamma_{m}^{(2)} \phi_{m}^{2} + \cdots \right]$$

$$\times \mathscr{N}_{o} \exp \left[-\frac{1}{2!} \int_{\vec{q}} \left\{ \Gamma_{o}^{(2)} - 2 \left(\chi + \frac{2\pi}{9} \left(\frac{\Theta_{P}}{T} \right)^{2} g \right) + \frac{2\pi}{9} \left(\frac{\Theta_{P}}{T} \right)^{2} h \left(q\ell \right)^{2} \right\} \left(\phi_{g} + \sum_{m=1}^{\infty} \phi_{m} \right)^{2} + \cdots \right]. \tag{54}$$

D. Associative chemical equilibria and weight distributions

We have constructed the partition function for a distribution $(m_g, n_1, n_2, ...)$ of associations and the gel. In general, there are enormous possible distributions (\mathcal{W}) if they preserve the number of polyzwitterions n_p ,

$$m_g + \sum_{m=1}^{\infty} m n_m = n_p. \tag{55}$$

Toward seeking an optimal distribution (\mathcal{W}^*), we combine Eqs. (51) and (55) to write the general partition function as

$$\mathbb{Q} = \sum_{\mathcal{W} = \{m_g, n_1, n_2, \dots\}} \delta \left[m_g + \sum_{m=1}^{\infty} m n_m - n_p \right]$$

$$\times \exp \left(-m_g \frac{\mu_g}{k_B T} - \sum_{m=1}^{\infty} n_m \left(-\ln mN - 1 + \frac{\mu_m}{k_B T} \right) \right) \mathbb{Z}_{\mathcal{W}} \delta \mathbb{Z}_{\mathcal{W}}$$

$$= \sum_{\mathcal{W} = \{m_g, n_1, n_2, \dots\}} \int \frac{d\theta}{2\pi} \exp \left(i\theta \left(n_g + \sum_{m=1}^{\infty} m n_m - n_p \right) \right)$$

$$\times \exp \left(-m_g \frac{\mu_g}{k_B T} - \sum_{m=1}^{\infty} n_m \left(-\ln mN - 1 + \frac{\mu_m}{k_B T} \right) \right) \mathbb{Z}_{\mathcal{W}} \delta \mathbb{Z}_{\mathcal{W}},$$
(56)

where $\mathbb{Z}_W\delta\mathbb{Z}_W$ are defined as in Eq. (51) for a specific distribution \mathscr{W} . The second equality arises from the integral representation of the Kronecker delta function $\delta[n]=\int\!d\theta/2\pi\,\exp{(i\,\theta\,n)}$. Once the free energies μ_g and μ_m are assigned in the mean-field percolation theory, the optimal distribution \mathscr{W}^* corresponds to the saddle point in the thermodynamic limit. Hence,

$$\mathbb{Q} \approx \mathbb{Q}^{*}$$

$$\equiv \exp\left(i\theta^{*}\left(m_{g}^{*} + \sum_{m=1}^{\infty} mn_{m}^{*} - n_{p}\right) - m_{g}^{*} \frac{\mu_{g}}{k_{B}T}\right)$$

$$- \sum_{m=1}^{\infty} n_{m}^{*}\left(\frac{\mu_{m}}{k_{B}T} - \ln mN - 1\right)\overline{\mathbb{Z}}_{\mathscr{W}^{*}} \delta\mathbb{Z}_{\mathscr{W}^{*}}.$$
(57)

To derive \mathcal{W}^* , by substituting Eq. (53), we differentiate $-\ln \mathbb{Q}^*$ with respect to \mathcal{W} and θ , leading to

$$-\left.\frac{\partial \ln \mathbb{Q}^*}{\partial (i\theta)}\right|_{\mathcal{W}^*, \alpha^*} \approx m_g^* + \sum_{m=1}^{\infty} m n_m^* - n_p = 0, \tag{58}$$

$$-\frac{1}{m} \frac{\partial \ln \mathbb{Q}^{*}}{\partial n_{m}} \bigg|_{\mathcal{W}^{*}, \theta^{*}} \approx -i\theta^{*} + \frac{\mu_{m}/k_{B}T - \ln mN + \ln \overline{\phi}_{m}^{*}}{m} + N \frac{\partial}{\partial \Omega} \left(\frac{\Omega \overline{f}_{\mathcal{W}^{*}}}{k_{B}T} \right) = 0, \tag{59}$$

$$-\left.\frac{\partial \ln \mathbb{Q}^*}{\partial m_g}\right|_{\mathcal{W}^*,\theta^*} \approx -i\theta^* + \frac{\mu_g}{k_B T} + N \frac{\partial}{\partial \Omega} \left(\frac{\Omega \bar{f}_{\mathcal{W}^*}}{k_B T}\right) = 0, \quad (60)$$

where $\overline{\phi}_m^*$ is the optimal homogenous concentration of m-associations, and the contribution of $\delta \mathbb{Z}_{\mathscr{W}}$ is not significant when the system is outside the Ginzburg critical region. Equation (58) is the mass conservation,

$$\overline{\phi}_g^* + \sum_{m=1}^{\infty} \overline{\phi}_m^* = \overline{\phi}, \tag{61}$$

which is independent of \mathcal{W} . Equation (59) is the condition of the chemical equilibrium among associations,

$$\frac{\mu_1}{k_B T} - \ln N + \ln \overline{\phi}_1^* = \dots = \frac{\mu_m / k_B T - \ln mN + \ln \overline{\phi}_m^*}{m}.$$
 (62)

The substitution of Eq. (24) for μ_m into Eq. (62) yields the well-known Stockmayer weight distribution, ^{2,26}

$$\frac{\exp\left(-\frac{f_{\text{bind}}}{k_B T}\right)}{N}\overline{\phi}_m^* = m\,\omega_m \left[\exp\left(-\frac{f_{\text{bind}}}{k_B T}\right)\overline{\phi}_1^*\right]^m,\tag{63}$$

with

$$\omega_m = \frac{(Nm - m)!}{m!(Nm - 2m + 2)!}.$$
(64)

Equation (60) is equivalent to the gelation condition. If a gel does exist, $\overline{\phi}_1^*$ must satisfy

$$\frac{\mu_g}{k_B T} + \ln N = \frac{\Delta \mu_{\text{loop}}}{k_B T} + \frac{f_{\text{bind}}}{k_B T} - \ln \left(\frac{(N-1)^{N-1}}{(N-2)^{N-2}} \right) = \ln \overline{\phi}_1^*, \quad (65)$$

where Eq. (28) is substituted. It is worth noting once again that $\Delta\mu_{\rm loop}$ is zero at the gelation points and becomes negative if loops are present within the gel. This equation clearly illustrates the fact that the presence of loops leads to an enhanced accumulation of polyzwitterion chains from the solution phase. Furthermore, the threshold value $\overline{\phi}_{1,\rm th}^*$ can be decided by substituting $\Delta\mu_{\rm loop}=0$ into Eq. (65). We can convert the threshold $\overline{\phi}_{1,\rm th}^*$ into the threshold concentration $\overline{\phi}_{\rm th}^*$. To derive the threshold value $\overline{\phi}_{\rm th}^*$, we parameterize

$$\exp\left(-\frac{f_{\text{bind}}}{k_B T}\right)\overline{\phi}_1^* = p(1-p)^{N-2},\tag{66}$$

and p satisfies

$$p = \frac{\sum_{m=1}^{\infty} 2(m-1) \overline{\phi}_m^*/mN}{\sum_{m=1}^{\infty} \overline{\phi}_m^*},$$
 (67)

as shown in Appendix B (supplementary material). Thus, p is the ratio of the number of associating monomers to the total number of monomers, corresponding to the extent of reaction of bindings. Moreover, the concentration of the associations is equal to

$$\sum_{m=1}^{\infty} \overline{\phi}_m^* = \frac{p}{(1-p)^2} \exp\left(\frac{f_{\text{bind}}}{k_B T}\right), \tag{68}$$

which is also $\overline{\phi}$ in the pregel regime. By substituting Eq. (66) into Eq. (65), we find the threshold $p_{\rm th}$ for the gelation as

$$p_{\rm th} = \frac{1}{N - 1}. (69)$$

Within a gel, the number of cross-links in one polyzwitterion chain is not less than 2, resulting in the average number of cross-links being more than one. Utilizing Eqs. (68) and (69), we determine the threshold concentration as

$$\overline{\phi}_{\rm th}^* = \frac{N-1}{(N-2)^2} \exp\left(\frac{f_{\rm bind}}{k_B T}\right). \tag{70}$$

Thus, a decrease in the temperature and an increase in the number of associative groups *N* facilitate the formation of the gel.

As a result, W^* in the pregel regime satisfies

$$\mathscr{W}_{\text{pregel}}^{\star}: \left\{ \overline{\phi}_{g}^{\star} = 0, \sum_{m=1}^{\infty} \overline{\phi}_{m}^{\star} = \overline{\phi} \mid \overline{\phi} \leq \overline{\phi}_{\text{th}}^{\star} \right\}.$$
 (71)

If $\overline{\phi}$ goes beyond the threshold value, the concentration of associations $\Sigma \overline{\phi}_m^*$, referred to as the "sol" concentration in this work, cannot be larger than $\overline{\phi}_{\rm th}^*$ because of the chemical equilibriums between the sol and the gel. According to Eq. (65), Stockmayer's treatment, assuming tree-like gel structures, leads to a static $\overline{\phi}_1^*$ in the postgel regime, hence a constant sol fraction and a linear growth of the gel fraction as $\overline{\phi}$ increases. The number distribution satisfies

$$\mathscr{W}_{\text{postgel,Stockmayer}}^{*}: \left\{ \overline{\phi}_{g}^{*} = \overline{\phi} - \overline{\phi}_{\text{th}}^{*}, \sum_{m=1}^{\infty} \overline{\phi}_{m}^{*} = \overline{\phi}_{\text{th}}^{*} \quad \middle| \quad \overline{\phi} > \overline{\phi}_{\text{th}}^{*} \right\}. \tag{72}$$

In contrast, by following Flory's approach, we introduce a shadow root $p_{\rm Flory}$, which satisfies

$$p_{\text{Flory}}(1-p_{\text{Flory}})^{N-2} = p(1-p)^{N-2},$$
 (73)

where p is the extent of reaction of the sol from Eq. (67), and

$$\overline{\phi} = \frac{p_{\text{Flory}}}{(1 - p_{\text{Flory}})^2} \exp\left(\frac{f_{\text{bind}}}{k_B T}\right). \tag{74}$$

As $\overline{\phi}$ increases in the postgel regime, p_{Flory} becomes larger, resulting in a smaller p and, consequently, a lower $\overline{\phi}_1^*$. According to Eq. (65), it implies the formation of loops in the gel, and the approach results

in a decreasing sol fraction and a nonlinear growth of the gel fraction as $\overline{\phi}$ increases. The number distribution satisfies

$$\mathcal{W}_{\text{postgel,Flory}}^{*}: \left\{ \overline{\phi}_{g}^{*} = \left(\frac{p_{\text{Flory}}}{(1 - p_{\text{Flory}})^{2}} - \frac{p}{(1 - p)^{2}} \right) \right.$$

$$\times \exp\left(\frac{f_{\text{bind}}}{k_{B}T} \right) \left| \overline{\phi} > \overline{\phi}_{\text{th}}^{*} \right\}. \tag{75}$$

E. Mean-field free energy, correlation functions, and the Ginzburg criterion

With an understanding of the interactions and the thermal response of weight distributions in the solution, we can naturally derive the free energy to predict thermoreversible phase behavior. By substituting Eqs. (53), (63), and (65) into Eq. (57), the mean-field free energy is

$$\frac{\overline{f}_{MF}}{\overline{k}_{B}T} \equiv \frac{-\ln\left(\mathbb{Q}/\delta\mathbb{Z}_{\mathscr{W}^{*}}\right)}{\Omega}$$

$$= \overline{\rho}_{c} \ln \overline{\rho}_{c} + \overline{\rho}_{a} \ln \overline{\rho}_{a} - \frac{\kappa^{3}\ell^{3}}{12\pi} + \frac{\overline{\phi}}{N} \ln \overline{\phi}$$

$$+ (1 - \overline{\phi}) \ln(1 - \overline{\phi}) + \chi \overline{\phi}(1 - \overline{\phi})$$

$$+ \frac{2\pi}{9} \left(\frac{\Theta_{P}}{T}\right)^{2} g(\kappa \ell) \overline{\phi}(1 - \overline{\phi}) + \frac{\overline{\phi}}{N} \ln \frac{\overline{\phi}_{1}^{*}}{\overline{\phi}}$$

$$- \sum_{n=1}^{\infty} \frac{\overline{\phi}_{m}^{*}}{mN} - \frac{\ln N}{N} \overline{\phi}, \tag{76}$$

where the first line is the common Flory–Huggins theory and the second line is the contributions from dipoles. The result is similar to previous research, ^{2,32,42} except for the linear term $\ln N/N \,\bar{\phi}$ of no physical effect.

The contribution of $\delta \mathbb{Z}_{\mathscr{W}^*}$ is not considerable unless the monomers are highly correlated in a long-range distance, leading to a strong fluctuation. To estimate fluctuations, we evaluate the segment–segment correlation function. By inserting the identity

$$1 = \int \mathscr{D}\{\phi\} \prod_{\vec{q} \neq \vec{0}} \delta \left[\phi - \phi_g - \sum_{m=1}^{\infty} \phi_m \right]$$
$$= \int \mathscr{D}\{\phi\} \mathscr{D}\{\lambda\} \exp \left[i \int_{\vec{q}} \lambda \left(\phi - \phi_g - \sum_{m=1}^{\infty} \phi_m \right) \right], \quad (77)$$

where λ is a Lagrangian multiplier field, into Eq. (54) under the random phase approximation (RPA), we get

$$\delta \mathbb{Z}_{\mathscr{W}} = \mathscr{N}_{o} \int \mathscr{D} \{\phi\} \exp \left[-\frac{1}{2!} \int_{\vec{q}} \left\{ \left[\Gamma_{o}^{(2)} - 2 \left(\chi + \frac{2\pi}{9} \left(\frac{\Theta_{P}}{T} \right)^{2} g \right) \right] + \frac{2\pi}{9} \left(\frac{\Theta_{P}}{T} \right)^{2} h q^{2} \right\} \phi^{2} \right] \int \mathscr{D} \{\lambda\} \exp \left[i \int_{\vec{q}} \lambda \phi \right] \mathscr{N}_{g}$$

$$\times \int \mathcal{D} \{\phi_g\} \exp \left[-\frac{1}{2!} \int_{\vec{q}} \Gamma_g^{(2)} \phi_g^2 - i \int_{\vec{q}} \lambda \phi_g \right]$$

$$\times \prod_{m=1}^{\infty} \mathcal{N}_m \int \mathcal{D} \{\phi_m\} \exp \left[-\frac{1}{2!} \int_{\vec{q}} \Gamma_m^{(2)} \phi_m^2 - i \int_{\vec{q}} \lambda \phi_m \right].$$
(78)

These integrals are the standard Gaussian integral; hence,

$$\delta \mathbb{Z}_{\mathscr{W}} = \mathscr{N}_o \mathscr{N}_p \int \mathscr{D} \{\phi\} \exp \left[-\frac{1}{2!} \int_{\vec{q}} \left\{ \frac{1}{\left(\Gamma_g^{(2)}\right)^{-1} + \sum_{m=1}^{\infty} \left(\Gamma_m^{(2)}\right)^{-1} + \Gamma_o^{(2)} \right. \right.$$
$$\left. -2\left(\chi + \frac{2\pi}{9} \left(\frac{\Theta_P}{T}\right)^2 g\right) + \frac{2\pi}{9} \left(\frac{\Theta_P}{T}\right)^2 h \left(q\ell\right)^2 \right\} \phi^2 \right], \tag{79}$$

where

$$\mathcal{N}_{p} = \int \mathcal{D}\{\phi\} \exp \left[-\frac{1}{2!} \int_{\vec{q}} \frac{\phi^{2}}{\left(\Gamma_{g}^{(2)}\right)^{-1} + \sum_{m=1}^{\infty} \left(\Gamma_{m}^{(2)}\right)^{-1}} \right].$$
 (80)

Consequently, the inverse correlation function $I^{-1}(q)$ equals

$$I^{-1}(q) = \frac{1}{\left(\Gamma_g^{(2)}\right)^{-1} + \sum_{m=1}^{\infty} \left(\Gamma_m^{(2)}\right)^{-1}} + \Gamma_o^{(2)}$$
$$-2\left(\chi + \frac{2\pi}{9} \left(\frac{\Theta_P}{T}\right)^2 g\right) + \frac{2\pi}{9} \left(\frac{\Theta_P}{T}\right)^2 h \left(q\ell\right)^2, \tag{81}$$

where $\Gamma_g^{(2)}$ is infinite in the pregel regime because of $\overline{\phi}_g = 0$. If a gel is present, $\Gamma_g^{(2)}$ will be infinite under Stockmayer's treatment because the mesh size of a tree-like gel is infinite. However, in practical scenarios, gels do not exhibit a strictly tree-like structure. In Flory's treatment, the gel structure is left unspecified, even though it allows for the formation of loops. Due to the lack of knowledge about the gel structure, we will discuss the correlation function outside the post-gel regime under both treatments in this paper. In the pregel regime, by employing Eqs. (39) and (45), the inverse correlation function approximates to

$$I^{-1}(q) \approx \varepsilon + Q q^2 + O(q^4) \tag{82}$$

around q = 0. Here,

$$\varepsilon = \frac{1}{\langle m \rangle_{u} N \overline{\phi}} + \frac{1}{1 - \overline{\phi}} - 2 \left(\chi + \frac{2\pi}{9} \left(\frac{\Theta_P}{T} \right)^2 g(\kappa \ell) \right), \tag{83}$$

$$Q = \frac{\left\langle mR_g^2(m)\right\rangle_w/\left\langle m\right\rangle_w}{3\left\langle m\right\rangle_wN\overline{\phi}} + \frac{2\pi}{9}\left(\frac{\Theta_P}{T}\right)^2h(\kappa\ell)\ell^2,\tag{84}$$

where the weight average over associations is defined as

$$\langle f \rangle_{w} \equiv \frac{\sum_{m=1}^{\infty} f \, \overline{\phi}_{m}^{*}}{\sum_{m=1}^{\infty} \overline{\phi}_{m}^{*}}.$$
 (85)

For example, according to the properties of Stockmayer's distributions in Appendix B (supplementary material),

$$\langle m \rangle_w = \frac{1+p}{1-p/p_{\rm th}}.$$
 (86)

The correlation length ξ equals

$$\xi^2 \equiv Q/\varepsilon.$$
 (87)

One reason to validate the mean-field (Flory–Huggins) theory is the multiplicity of the interactions.⁴³ In a solution, each polymer is surrounded by many other polymers and interacts with them simultaneously. In other words, the net interaction of the polymer has been ensemble averaged. Consequently, if the segments strongly correlate with each other over a long distance, which exceeds the size of the polymer, or the association in our case, the net interaction of a polymer cannot be effectively averaged within the polymer itself. This leads to a breakdown of the mean-field theory when critical behaviors dominate the system. Based on this argument, the Ginzburg criterion is

$$\frac{\xi^{2}}{\langle mR_{g}^{2}(m)\rangle_{w}/\langle m\rangle_{w}} \gg 1 \implies \varepsilon \ll \frac{1}{\langle m\rangle_{w}N\overline{\phi}} + \frac{\frac{2\pi}{3}\left(\frac{\Theta_{p}}{T}\right)^{2}h(\kappa\ell)\ell^{2}}{\langle mR_{g}^{2}(m)\rangle_{w}/\langle m\rangle_{w}}, \tag{88}$$

agreeing with the previous research.⁴⁴⁻⁴⁶ As the system approaches the critical points $\varepsilon \to 0$, the fluctuations inevitably ruin the RPA. We will address this issue using the RG theory in Sec. IV.

IV. RESULTS

The chemical properties of monomer determine the mixing parameter χ . We assume that the polyzwitterion follows the UCST behavior and assign χ to

$$\chi = \left(\frac{1}{2} + \frac{1}{\sqrt{N}} + \frac{1}{2N}\right) \frac{\Theta_{\text{FH}}}{T},\tag{89}$$

where Θ_{FH} will be the critical temperature if there is no dipole interaction. In addition, we assign the following values: N = 100, $\ell_B/\ell = 0.988 \ \Theta_{\rm FH}/T, \ \Theta_p/\Theta_{\rm FH} = 0.75, \ {\rm and \ a \ temperature \ range \ of}$ $T/\Theta_{\rm FH}$ = 1.4–1.7. If $\Theta_{\rm FH}$ is equal to 200 K, we can map the system into the polyzwitterions of Kuhn length $\ell \approx 1$ nm carrying $p \approx 42D$ ≈ 0.87e nm, corresponding to side chemical groups roughly having six (C-C) covalent bonds, dissolving in an aqueous solution $(\varepsilon_r \approx 80)$ within the temperature range 280–340 K. Using the meanfield free energy presented in Eq. (76), we derive the osmotic pressure and the chemical potential of the polyzwitterion solution. Macrophase separation occurs when the osmotic pressure and the chemical potential are the same as in two phases. Gelation occurs if the concentration exceeds the threshold concentration $\overline{\phi}_{th}^*$ as defined in Eq. (70). For illustrative purposes, we provide phase diagrams in the $\overline{\phi}$ – T plane for a salt-free polyzwitterion solution with increasing exp $(\Delta s/k_B)$ = 0.03 ~ 0.08 in Fig. 1. To explore the effect of salt with changes in temperature, we depict the same phase diagrams for $\overline{\rho}_{\text{salt}}$ = 0.01 in Fig. 2. In addition, to investigate the effect of varying

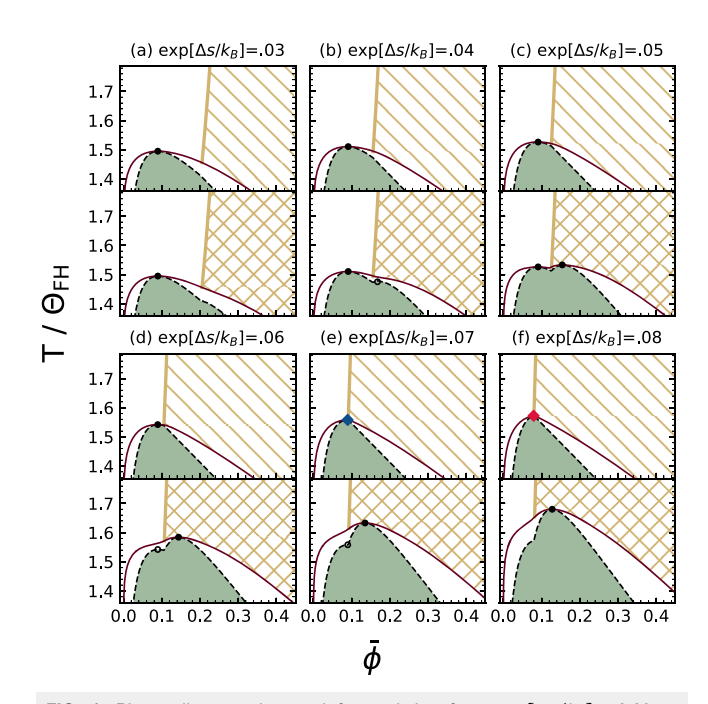


FIG. 1. Phase diagrams in a salt-free solution from $\exp\left[\Delta s/k_B\right]=0.03$ to $\exp\left[\Delta s/k_B\right]=0.08$, corresponding to (a)–(f). The top (bottom) panel in each plot is the phase diagram under Stockmayer's (Flory's) treatment. Here, the red solid lines represent the binodal curve, the black dashed lines indicate the spinodal curves, the green-shaded regions denote the unstable regions, the yellow solid line marks the gelation line, and the diagonal-hatched (cross-hatched) regions show the gel phase under Stockmayer's (Flory's) treatment. The critical points are indicated by black solid circles, and the pseudo-critical points under Flory's treatment are shown as empty circles. The bicritical point is marked as a blue (red) solid diamond if $\partial \varepsilon/\partial \bar{\phi}=0$ ($\neq 0$).

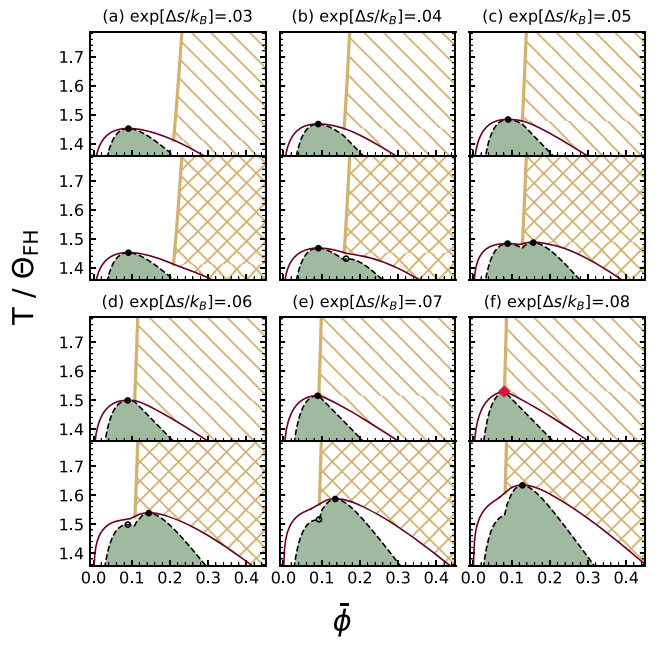


FIG. 2. Same as Fig. 1 for $\overline{\rho}_{salt} = 0.01$.

salt concentrations, we also present phase diagrams in the $\overline{\phi} - \overline{\rho}_{salt}$ plane at $\Theta_{FH} = 1.45$ in Fig. 3. Here, the electric neutrality ensures $\overline{\rho}_c = \overline{\rho}_a = \overline{\rho}_{salt}$.

We will discuss Stockmayer's and Flory's treatments separately. In addition, to clarify our terminology, we refer to

- (i) the intersection of the binodal line and the spinodal line as a critical point, and the symbols $\overline{\phi}_c^*$ and T_c denote the corresponding concentration and temperature, respectively.
- (ii) the intersection of the gelation line and the binodal line as a tricritical point, 47 and the symbols $\overline{\phi}_{\rm tri}^*$ and $T_{\rm tri}$ denote the corresponding concentration and temperature, respectively.
- (iii) the intersection of the gelation line and the spinodal line as a bicritical point,⁴⁷ and the symbols $\overline{\phi}_{bi}^*$ and T_{bi} denote the corresponding concentration and temperature, respectively.

A. Under Stockmayer's treatment

At first, we observe that macrophase separation occurs at a temperature higher than Θ_{FH} , indicating an increasing propensity for MPS due to dipole–dipole interactions. Furthermore, we notice two scenarios regarding the interplay between MPS and gelation.

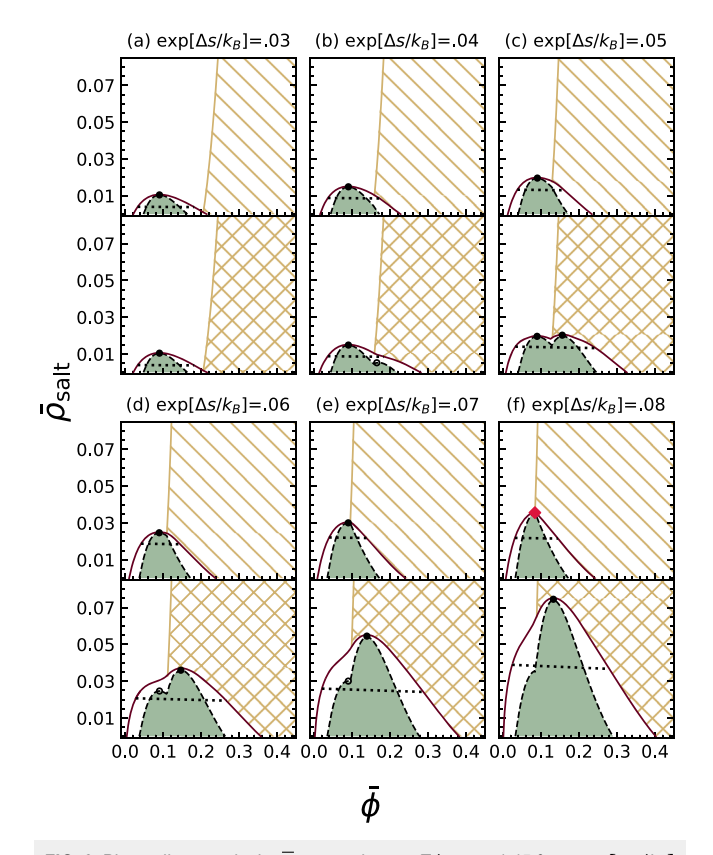


FIG. 3. Phase diagrams in the $\overline{\phi} - \overline{\rho}_{\text{salt}}$ plane at $T/\Theta_{\text{FH}} = 1.45$ from $\exp\left[\Delta s/k_{B}\right] = 0.03$ to $\exp\left[\Delta s/k_{B}\right] = 0.08$, corresponding to (a)–(f). The dotted lines are tie lines, and the meaning of other lines, dots, and shaded regions are the same as the description in Fig. 1. In panel (e), the critical point in the upper panel is in the pregel regime.

In the first scenario, MPS facilitates gelation. When the solution is initially homogeneous, as the temperature decreases, it undergoes MPS, leading to polymer-rich droplets, where gelation can occur if the droplets are more concentrated than the threshold concentration. The second scenario shows that gelation facilitates MPS as well. When there is a homogeneous gel phase at a high temperature, as the temperature decreases, the gel will absorb more flowing polyzwitterions and expel the polymer-poor liquid. The interplay between MPS and gelation becomes more significant as $\exp(\Delta s/k_B)$ increases because cross-links are easier to form. In saline solutions, ions break the cross-links and dissolve polymer-rich and gel phases. Therefore, the MPS and gelation occur at lower temperatures, as shown in Fig. 2. In addition, the slopes of tie lines are negative, as depicted in Fig. 3. It is worth noting that there is no shadow curve, which is a common phenomenon in polydisperse solutions. 48,49

Moreover, we observe the interesting movements of the critical and tricritical points. At exp $(\Delta s/k_b)$ = 0.03, the critical point is located around the overlap concentration $1/\sqrt{N}$ and remains significantly distant from the tricritical point. We expect that the critical behaviors of the two points remain within their respective universality classes. However, as $\exp(\Delta s/k_B)$ increases, the value of $\overline{\phi}_{c}^{*}$ remains close to $1/\sqrt{N}$, while $\overline{\phi}_{tri}^{*}$ gets closer, eventually merging into a bicritical point at $\exp(\Delta s/k_B) = 0.07$, as illustrated in Fig. 1(e). The value exp $(\Delta s/k_B)$ = 0.07 is derived from the analytical calculation of $\overline{\phi}_{c}^{*}$ shown in Appendix C (supplementary material). As $\exp(\Delta s/k_B)$ increases further, the bicritical point moves to the lower concentration. It is worth noting that $\partial \varepsilon / \partial \overline{\phi} \mid_{\overline{\phi} = \overline{\phi}_{\bullet}^{*}} \neq 0$ when $\exp{(\Delta s/k_B)} > 0.07.$

1. Merger of two universality classes

MPS belongs to the Ising universality class, whereas gelation falls into a percolation universality class. When the critical and tricritical points merge into the bicritical points, they must exhibit only one kind of critical behaviors. It implies a crossover from two distinct universality classes to a merged universality class. When the critical point is far from the tricritical point, we can renormalize the fluctuations caused by macrophase separation within the Ginzburg region. By applying the RG technique of the ϕ^4 theory, correlation function is renormalized into

$$\xi^2 = \frac{Q}{\varepsilon^{2\nu}},\tag{90}$$

and the Fisher approximation 54,55 of correlation functions is given by

$$I^{-1}(q) = Q(q^2 + \xi^{-2})^{1-\eta/2}, \tag{91}$$

where ε and Q are defined as in Eqs. (83) and (56), respectively. Since the concentration field undergoing MPS is not equivalent to the total concentration field ϕ , the validity of Eqs. (90) and (91) is doubtful. However, a careful analysis in Appendix D (supplementary material) demonstrates that the strongest fluctuations dominate the system, thereby validating Eqs. (90) and (91).

As the tricritical points get closer and closer to the critical points, the impact on Q becomes significant because $\langle mR_g(m)\rangle_w$ and $\langle m \rangle_w$ are divergent. Renormalizing Q is inevitable and raises doubts about the validity of Eqs. (90) and (91). We are unsure how to perform RG for MPS and gelation simultaneously. It is also uncertain whether we can perform RG separately for MPS and gelation. Nevertheless, we follow M.E. Fisher's suggestion, which states that "the nature of the transition and the critical point remains ideal if observed at a fixed force f,"56 which has been applied to three-component liquid mixtures,⁵⁷ resulting in the assumption that Eqs. (90) and (91) remain valid even near the gelation points. We need to perform RG for gelation, and, according to the ϕ^3 theory, ⁵⁰ the renormalized Q exhibits

$$\frac{\left\langle mR_g^2(m)\right\rangle_w/\langle m\rangle_w}{3\langle m\rangle_wN\overline{\phi}} \sim \left(1 - \frac{p}{p_{\rm th}}\right)^0 \text{ (percolation theory)}, (92)$$

which has been confirmed in the simulations for cubic lattices⁶⁰ and polymer melts.²⁴ Both $\langle mR_g(m)\rangle_w$ and $\langle m\rangle_w$ diverge, but their ratio does not diverge. However, Eq. (92) does not apply to our model. These theories and simulations do not include the excluded volume effect. They are suitable only for concentrated solutions where the excluded volume interaction is screened. Although the critical points are located at the overlap concentration $\overline{\phi}_{c}^{*} \sim 1/\sqrt{N}$, this is the overlap concentration for a single polyzwitterion, not for the associations! In cases where the excluded volume interaction is partially screened, according to the Flory-de Gennes theory, 25,61 the fractal structure of characteristic associations follows $R_g(m) \sim (mN)^{2/(2+d)}$. It implies that the overlap concentration at d = 3 is

$$\frac{mN}{R_g^3(m)} \sim \frac{1}{(mN)^{1/5}} > \frac{1}{\sqrt{N}}.$$
 (93)

The excluded volume effect is not screened out for the associations, so we treat them as lattice animals. By following Flory's argument,25 the free energy of lattice animals approximates to

$$\frac{F}{k_B T} \sim \frac{R_g^2(m)}{(mN)^{1/2}} + w_{pp} \frac{(mN)^2}{R_g^d(m)},\tag{94}$$

thereby giving

$$R_g(m) \sim (mN)^{\frac{5}{2(2+d)}}$$
 (95)

from energy minimization, where d = 3. As for the number distribution, because the associations are porous, we continue assuming that they are tree-like. As a result, Q follows

$$Q \approx \frac{\left\langle mR_g^2(m)\right\rangle_w/\left\langle m\right\rangle_w}{3\left\langle m\right\rangle_wN\overline{\phi}} \sim \left(1 - \frac{p}{p_{\text{th}}}\right)^{4\nu_f - 1} \text{ (our model)}, \qquad (96)$$

where $v_f = 5/2(2+d) = 1/2$, and we derive the divergent behavior of Q from formulas in Appendix B (supplementary material). Similarly, we apply the same argument at tricritical points.

2. Crossover critical behaviors

To demonstrate the merger of the two universality classes, we focus on the divergence behaviors as $T \rightarrow T_c$ at the critical points. As $T \rightarrow T_c$, by its definition, ε approaches to zero. Simultaneously, Q also becomes larger because there are more large associations at a lower temperature. Similarly, as $T \rightarrow T_{\rm tri}$, Q diverges and ε also becomes smaller at a lower temperature. The corresponding scaling laws are

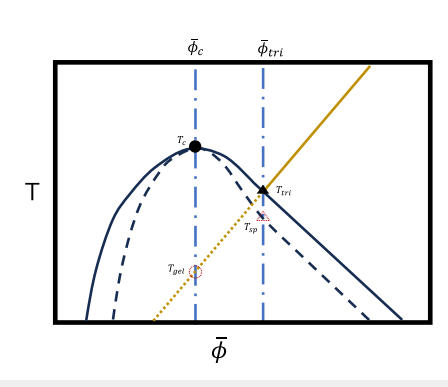


FIG. 4. Schematic presentation of the definitions of T_{qel} and $T_{\text{sp.}}$

$$\begin{cases} \varepsilon \sim \frac{1}{T} - \frac{1}{T_{\rm c}}, Q \sim \left(\frac{1}{T} - \frac{1}{T_{\rm gel}(\overline{\phi}_{\rm c}^*)}\right)^{-(4\nu_f - 1)}, & \text{critical points,} \\ \varepsilon \sim \frac{1}{T} - \frac{1}{T_{\rm sp}(\overline{\phi}_{\rm c})}, Q \sim \left(\frac{1}{T} - \frac{1}{T_{\rm tri}}\right)^{-(4\nu_f - 1)}, & \text{tricritical points,} \end{cases}$$
(9

where $T_{\rm gel}(\overline{\phi}_c^*)$ is the temperature of the gelation point at $\overline{\phi}_c^*$, $T_{\rm sp}(\overline{\phi}_c)$ is the temperature of the spinodal point at $\overline{\phi}_{\rm tri}^*$, and the scaling law of Q is from $p-p_{\rm th}\sim T-T_{\rm gel}$. The schematic presentation of these temperatures is shown in Fig. 4.

Because the scaling laws of Q and ε are relative to different temperatures, there is no well-defined critical exponent. Instead, we define the apparent critical exponents at the temperature T as

$$v_{\text{app}} = -\frac{\partial \ln \xi}{\partial \ln \left(\frac{1}{T_{\text{c(tri)}}} - \frac{1}{T}\right)} \bigg|_{T} = v \frac{\partial \ln \varepsilon}{\partial \ln \left(\frac{1}{T_{\text{c(tri)}}} - \frac{1}{T}\right)} \bigg|_{T}$$
$$-\frac{1}{2} \frac{\partial \ln Q}{\partial \ln \left(\frac{1}{T_{\text{c(tri)}}} - \frac{1}{T}\right)} \bigg|_{T}, \tag{98}$$

$$\gamma_{\text{app}} = -\frac{\partial \ln I(0)}{\partial \ln \left(\frac{1}{T_{c(\text{tri})}} - \frac{1}{T}\right)} \bigg|_{T} = (2 - \eta) \nu \frac{\partial \ln \varepsilon}{\partial \ln \left(\frac{1}{T_{c(\text{tri})}} - \frac{1}{T}\right)} \bigg|_{T} + \frac{\eta}{2} \frac{\partial \ln Q}{\partial \ln \left(\frac{1}{T_{c(\text{tri})}} - \frac{1}{T}\right)} \bigg|_{T},$$
(99)

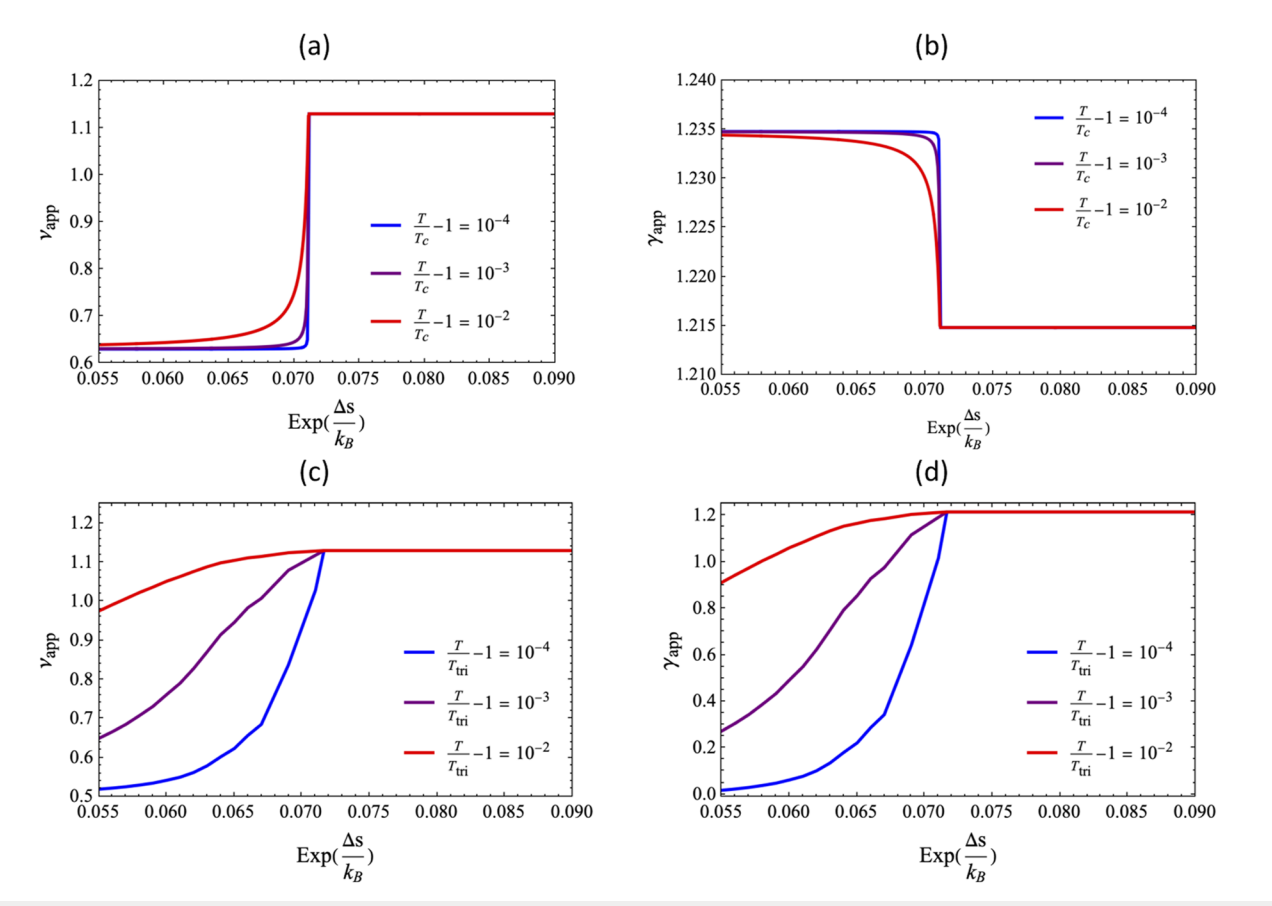


FIG. 5. Given v = 0.63, $\eta = 0.04$, and $v_f = 0.5$, the apparent critical exponents for critical points are shown in (a) and (b), where T_c is the temperature of critical points. Similarly, the apparent critical exponents for tricritical points are shown in (c) and (d), where T_{tri} is the temperature of tricritical points. Once exp $(\Delta s/k_B) > 0.07$, the critical exponents converge into values of bicritical points. These values are evaluated in a salt-free solution.

where the second equality is derived from the substitution of Eqs. (90) and (91). $T_{\rm c}$ and $T_{\rm tri}$ denote the critical and tricritical temperatures, respectively. When the critical point and the tricritical points merge into the bicritical points, their apparent critical exponents merge into the critical exponents at the bicritical points. Substituting the scaling law equation (97) into $\nu_{\rm app}$ and $\gamma_{\rm app}$, we derive the first-order approximation of $\nu_{\rm app}$ and $\gamma_{\rm app}$ as

$$v_{\text{app}} \approx \begin{cases} v + \left(2v_f - \frac{1}{2}\right) \frac{\frac{1}{T_c} - \frac{1}{T}}{\frac{1}{T_{\text{gel}}} - \frac{1}{T}}, & \text{critical points,} \\ v \frac{\frac{1}{T_{\text{sp}}} - \frac{1}{T}}{\frac{1}{T_{\text{tri}}} - \frac{1}{T}} + \left(2v_f - \frac{1}{2}\right), & \text{tricritical points,} \end{cases}$$

$$v + \left(2v_f - \frac{1}{2}\right), & \text{bicritical points,} \end{cases}$$

$$\left(2 - \eta\right) v - \eta \left(2v_f - \frac{1}{2}\right) \frac{\frac{1}{T_c} - \frac{1}{T}}{\frac{1}{T_{\text{gel}}} - \frac{1}{T}}, & \text{critical points,} \end{cases}$$

$$\left(2 - \eta\right) v \frac{\frac{1}{T_{\text{sp}}} - \frac{1}{T}}{\frac{1}{T_{\text{tri}}} - \frac{1}{T}} - \eta \left(2v_f - \frac{1}{2}\right), & \text{tricritical points,} \end{cases}$$

$$\left(2 - \eta\right) v - \eta \left(2v_f - \frac{1}{2}\right), & \text{bicritical points.} \end{cases}$$

$$\left(2 - \eta\right) v - \eta \left(2v_f - \frac{1}{2}\right), & \text{bicritical points.} \end{cases}$$

$$\left(100\right)$$

We adopt the accepted values v = 0.63 and $\eta = 0.04.^{50}$ The apparent critical exponents for a salt-free solution are depicted in Fig. 5. The merger of two universality classes leads to crossover behaviors in $v_{\rm app}$ and $\gamma_{\rm app}$, especially when temperatures deviate significantly from $T_{\rm c}$ or $T_{\rm tri}$. At the bicritical point, where $\exp{(\Delta s/k_B)} > 0.07$, the v value is higher, resulting in enhanced $v_{\rm app}$. These anomalous enhancements in critical exponents have recently been observed in polyelectrolyte coacervate mixtures. For the $\gamma_{\rm app}$ values, those of the critical points experience a slight suppression, while those of the tricritical points exhibit a significant enhancement. Because geometric phase transitions do not significantly affect the second virial coefficient ε , in comparison with the critical points,

the tricritical points have a smaller γ , consistent with experimental observations. ⁶³ The presence of salt ions changes $T_{\rm c}$ and $T_{\rm tri}$, but the crossover behaviors remain similar because the Debye length is much smaller than ξ in critical phenomena. ⁶⁴

While we have explained that the crossover critical behaviors arise from merging two universality classes, the underlying microscopic mechanism remains a puzzle. To address this question, we must understand how fluctuations impact the associations. Intuitively, the associations are disassembled by small-scale fluctuations, leading to inhomogeneous concentrations. If the disassembly occurs, the energy of fluctuations will dissipate. Associations resist fluctuations that are smaller than themselves. Meanwhile, fluctuations at a large scale tend to move associations rather than disassembling them. Consequently, in comparison with an ideal Ising behavior, the correlation length ξ of an associative solution is shorter at temperatures above the critical point $(T > T_c)$. However, when the solution reaches the critical point, fluctuations are larger than any associations, resulting in ξ being the same as in the ideal Ising model. When we describe the divergence using a scaling law, $\xi \sim (T - T_c)^{-\nu_{app}}$, the apparent critical exponents must be enhanced, i.e., $v_{app} > v$. A schematic illustration of this phenomenon is shown in Fig. 6. Furthermore, we can support this argument with the fluctuation free energy, $\delta f \sim -1/\xi^3$. As ξ becomes shorter and shorter, leading to the suppression of large associations, δf becomes more negative. We provide a more detailed quantitative analysis in Appendix E (supplementary material). A similar argument can apply to the tricritical points.

It is worth noting that the crossover behaviors seem to suggest a transition to a new universality class at bicritical points. However, Fisher's method is an assumption and does not provide a rigorous analysis of the bicritical point. Anomalous critical exponents do not necessarily imply that the universality class changes; they can arise from narrow Ginzburg regions, as shown in the restricted primitive model 65,66 and the polymerization process. 67,68 For example, at the critical points of MPS in Fig. 5, the critical exponents deviate from the Ising model at a large $|T - T_c|$, where the correlation length ξ is not much larger than the characteristic associations. Moreover, we assume that the associations belong to lattice animals, while associations can exhibit different fractal structures at varying association

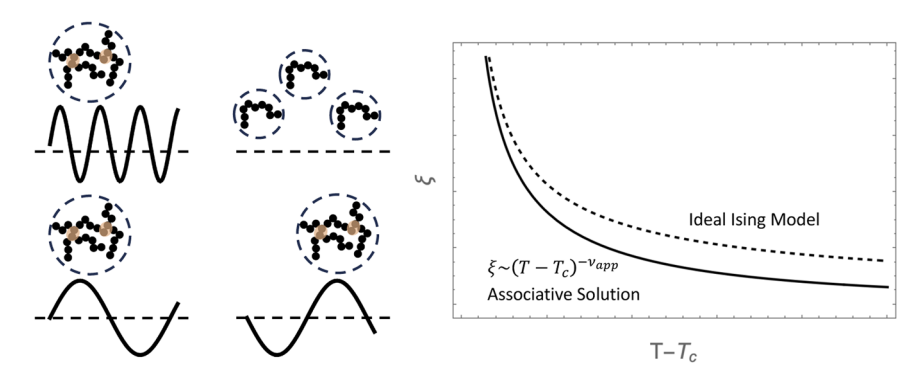


FIG. 6. If the scale of fluctuations is shorter than the associations, the fluctuations can disassemble the associations, and they dissipate after dissembling. Meanwhile, the associations move back and forth under the influence of large-scale fluctuations, but the fluctuations do not dissipate. Therefore, compared to the ideal Ising behavior, ξ is shorter in an associative solution at $T > T_c$. However, ξ is the same as the Ising one at $T = T_c$, so the apparent v_{app} is larger than v.

strengths, impacting virial coefficients, as demonstrated in the simulations of Stockmayer fluid^{69,70} and patch particle model.^{33,34,71,72} This variability adds another layer of complexity to analyzing the critical behavior at bicritical points. Conducting a rigorous analysis can lead to a more concrete conclusion about the universality class at bicritical points, and we will explore it in future work.

B. Under Flory's treatment

In contrast to Stockmayer's treatment, the presence of loops within the gel network in Flory's treatment results in a larger region for macrophase separation. The loops decrease the free energy and make the gel phase more resistant to ions, resulting in a more negative slope of tie lines in Fig. 3. Moreover, the loop formation can lead to a split of the gel into polymer-poor and polymer-rich gels, called gel-gel phase separation, because the loop formation in the polymer-rich gel lowers the total free energy if the binding strength is sufficiently strong, as depicted in Figs. 1(c)-1(f). These splits in the gel lead to binodal curves exhibiting a double-hill shape, and there are possibly two apexes on the spinodal curves. These two apexes are not always observable if one is situated below the binodal curves. We define the ones located beneath the binodal curves as pseudo-critical points. In the pregel regime, the concentrations and temperatures of the pregel apexes are the same as the critical points under Stockmayer's treatment. As the value of $\exp(\Delta s/k_B)$ increases, a new apex appears in the postgel regime. With further increases in exp ($\Delta s/k_B$), the temperature of the postgel apex continues rising while the corresponding concentration decreases. When $\exp(\Delta s/k_B) > 0.07$, the pregel apex no longer exists. We present the quantitative analysis of the emergence of these two apexes in detail in Appendix C (supplementary material).

There are critical and tricritical points under Flory's treatment in Fig. 1. As discussed earlier, the pregel critical and tricritical points exhibit anomalous critical behaviors. However, with $\exp{(\Delta s/k_B)} > 0.07$, no bicritical point emerges, making it impossible to observe the merger of two universality classes. Instead, a postgel critical point appears. The critical behavior of this postgel critical point is contingent on the gel structure, particularly $\Gamma_g^{(2)}$, which remains unspecified under Flory's treatment. We need a microscopic model that accounts for detailed structures. However, the presence of loops within the gel network introduces a complexity. A model accounting for loops within a gel network falls outside our scope, and we leave it in the future.

V. CONCLUSIONS

Employing the mean-field percolation theory and field theory formalism, we have developed a theory for solutions consisting of homo-polyzwitterions capable of forming tree-like associations and gels through pairwise dipole bindings. We have derived the system free energy and predicted the occurrence of thermoreversible macrophase separation (MPS) and gelation under various physical conditions, including dipole strength, hydrophobicity, dielectric property of the solvent, and ionic strength. When the gel forms, we have employed two conventional methods to describe the gel: (1) Stockmayer's treatment, where the gel resembles tree-like structures, and (2) Flory's treatment, where the formation of loops with the gel is allowed. The phase diagrams reveal that, as the temperature

decreases, the solution undergoes MPS, enhanced due to attractive interactions among dipoles. MPS can be a liquid-liquid phase separation. However, if the concentration of polymer-rich droplets exceeds a certain threshold, gel can form within the droplets, resulting in a gel-liquid phase separation. MPS can facilitate gelation in this case. Another scenario for gel-liquid phase separation occurs when gelation itself promotes MPS. Once the gel forms at a high concentration, decreasing the temperature causes the gel to incorporate more free polyzwitterions and expel the polymer-poor liquid. Both treatments exhibit these scenarios, but only Flory's treatment reveals an interesting gel–gel phase separation. The gel division benefits the free energy of the entire system because there can be more loops in the polymer-rich gel phase. The phase diagrams also exhibit the multiple critical points arising from the coupling of the MPS and gelation in the polyzwitterion solution.

In addition, with the help of the renormalization group theory, we have discovered anomalous critical behaviors near the critical, tricritical, and bicritical points. Under Stockmayer's treatment, the critical point remains distinct from the tricritical point when the binding entropy loss, $\Delta s = S_{\text{binding}} - S_{\text{unbinding}}$, is substantial. The tricritical and bicritical points belong to their respective universality classes. As the entropy loss decreases, the tricritical point moves closer to the critical point until it merges into a bicritical point, resulting in a critical behavior belonging to the universality class of bicritical points. Remarkably, their critical behaviors display a crossover to new critical behavior during this transition. From the apparent critical exponents in this limit, especially v_{app} , we discuss the emergent anomalous concentration fluctuations and argue that the microscopic mechanism behind these anomalies is the suppression of fluctuations during association-disassembly. In contrast, although anomalous critical behaviors appear under Flory's treatment, we cannot observe the merging process because there is no bicritical point. Instead, postgel critical points are present. The lack of knowledge regarding gel structures presents a challenge in investigating the critical behaviors of postgel critical points.

Our theory addresses the growing interest in polyzwitterions. It focuses on their thermoreversible properties and can explain the anomalous critical behaviors observed in recent experiments. 62 In addition, the proposed theoretical framework can be extended to various electrostatic interactions, enabling the investigation of the phases and formations of biomolecular condensates involving intrinsically disordered proteins. However, similar to most polyelectrolyte theories, the complexities associated with dissolved small electrolyte ions introduce challenges in making quantitative predictions, such as charge renormalization. Our discussion primarily focuses on the aggregations led by quadrupoles. However, dipoles can also contribute to the formation of aggregates involving quadrupoles and higher-order multipoles upon further cooling. These aggregates have more negative binding free energy, facilitating MPS and gelation and resisting concentration fluctuations more effectively. As a result, the phase diagram can exhibit a wilder binodal curve, a more inclined gel transition line, and a narrower Ginzburg region under the framework in this paper. Moreover, except for these quantitative modifications, their presence can result in more complicated self-assembled phases, such as micelles in a solute phase and fibers in a gel phase. Their impacts on phase transitions and critical behaviors raise a challenge in describing phase behaviors of charged associative polymer solutions. Addressing this

challenge goes beyond the scope of the present work, and we leave it for future investigations.

SUPPLEMENTARY MATERIAL

This article contains a supplementary material. We present the derivation of Landau-Ginzburg free energy in Appendix A, the Stockmayer distribution in Appendix B, the analysis of critical points in Appendix C, the ϕ^4 theory of the model in Appendix D, and the suppression of associations in Appendix E.

ACKNOWLEDGMENTS

The authors thank Shibananda Das for stimulating discussions. They acknowledge the National Science Foundation (Grant No. DMR 2309539) and AFOSR (Grant No. FA9550-23-1-0584) for the support.

AUTHOR DECLARATIONS

Conflict of Interest

The authors have no conflicts to disclose.

Author Contributions

Siao-Fong Li: Data curation (lead); Investigation (equal); Writing – original draft (lead). Murugappan Muthukumar: Conceptualization (lead); Project administration (lead); Writing - review & editing (equal).

DATA AVAILABILITY

The data that support the findings of this study are available within the article and its supplementary material.

REFERENCES

- ¹M. Muthukumar, Physics of Charged Macromolecules-Synthetic and Bological Systems (Cambridge University Press, 2023).

 F. Tanaka, Polymer Physics: Applications to Molecular Association and Thermore-
- versible Gelation (Cambridge University Press, 2011).
- ³F. Tanaka and M. Ishida, "Microphase formation in mixtures of associating polymers," Macromolecules 30, 1836–1844 (1997).

 D. Prusty, V. Pryamitsyn, and M. Olvera de la Cruz, "Thermodynamics of
- associative polymer blends," Macromolecules 51, 5918-5932 (2018).
- ⁵M. Rubinstein and A. N. Semenov, "Dynamics of entangled solutions of associating polymers," Macromolecules 34, 1058-1068 (2001).
- ⁶A. N. Semenov and M. Rubinstein, "Thermoreversible gelation in solutions of associative polymers. 1. Statics," Macromolecules 31, 1373-1385 (1998).
- ⁷F. Wurm, B. Rietzler, T. Pham, and T. Bechtold, "Multivalent ions as reactive crosslinkers for biopolymers—A review," Molecules 25, 1840 (2020).
- ⁸Z. Zhang, Q. Chen, and R. H. Colby, "Dynamics of associative polymers," Soft Matter 14, 2961-2977 (2018).
- ⁹J. F. Joanny, "Gel formation in ionomers," Polymer **21**, 71–76 (1980).
- 10 M. Muthukumar, "Localized structures of polymers with long-range interactions," J. Chem. Phys. 104, 691-700 (1996).
- 11 M. Muthukumar, "Ordinary-extraordinary transition in dynamics of solutions of charged macromolecules," Proc. Natl. Acad. Sci. U. S. A. 113, 12627-12632 (2016).

- ¹²M. Muthukumar, "50th anniversary perspective: A perspective on polyelectrolyte solutions," Macromolecules 50, 9528-9560 (2017).
- ¹³S. Adhikari, M. A. Leaf, and M. Muthukumar, "Polyelectrolyte complex coacervation by electrostatic dipolar interactions," J. Chem. Phys. 149, 163308
- ¹⁴D. Jia and M. Muthukumar, "Dipole-driven interlude of mesomorphism in polyelectrolyte solutions," Proc. Natl. Acad. Sci. U. S. A. 119, e2204163119 (2022).
- ¹⁵R. Kumar, B. G. Sumpter, and M. Muthukumar, "Enhanced phase segregation induced by dipolar interactions in polymer blends," Macromolecules 47, 6491-6502 (2014).
- 16 R. Kumar and G. H. Fredrickson, "Theory of polyzwitterion conformations," J. Chem. Phys. 131, 104901 (2009).
- ¹⁷A. B. Lowe and C. L. McCormick, "Synthesis and solution properties of zwitterionic polymers," Chem. Rev. 102, 4177-4190 (2002).
- ¹⁸K. Li and Q. Zhong, "Aggregation and gelation properties of preheated whey protein and pectin mixtures at pH 1.0-4.0," Food Hydrocolloids 60, 11-20 (2016).
- ¹⁹S. Kudaibergenov, W. Jaeger, and A. Laschewsky, "Polymeric betaines: Synthesis, characterization, and application," in Supramolecular Polymers Polymeric Betains Oligomers (Springer, 2006), pp. 157-224.
- ²⁰ A. E. Neitzel, G. X. De Hoe, and M. V. Tirrell, "Expanding the structural diversity of polyelectrolyte complexes and polyzwitterions," Curr. Opin. Solid State Mater. Sci. 25, 100897 (2021).
- ²¹L. Zheng, H. S. Sundaram, Z. Wei, C. Li, and Z. Yuan, "Applications of zwitterionic polymers," React. Funct. Polym. 118, 51-61 (2017).
- 22 F. Tanaka, "Intramolecular micelles and intermolecular crosslinks in thermoreversible gels of associating polymers," J. Non-Cryst. Solids 307-310, 688-697
- ²³K. Singh and Y. Rabin, "Aging of thermoreversible gel of associating polymers," Macromolecules 53, 3883-3890 (2020).
- $^{\bf 24}{\rm D.~T.~Li,~P.~E.}$ Rudnicki, and J. Qin, "Distribution cutoff for clusters near the gel point," ACS Polymers Au 2, 361-370 (2022).
- ²⁵D. Stauffer and A. Aharony, Introduction to Percolation Theory (Taylor & Francis, 2018).
- $^{\mathbf{26}}\mathrm{W}.$ H. Stockmayer, "Theory of molecular size distribution and gel formation in branched-chain polymers," J. Chem. Phys. 11, 45-55 (1943).
- ²⁷I. Y. Erukhimovich and A. Ermoshkin, "Statistical thermodynamics of the formation of an infinite cluster of thermally reversible chemical bonds," J. Exp. Theor. Phys. 88, 538 (1999).
- ²⁸P. J. Flory, *Principles of Polymer Chemistry* (Cornell University Press, 1953).
- ²⁹R. M. Ziff and G. Stell, "Kinetics of polymer gelation," J. Chem. Phys. 73,
- $^{\bf 30}$ P.-G. De Gennes, Scaling Concepts in Polymer Physics (Cornell University Press,
- ³¹D. Stauffer, A. Coniglio, and M. Adam, "Gelation and critical phenomena," in Polymer Networks (Springer, 2005), pp. 103-158.
- ³²F. Tanaka, "Theory of thermoreversible gelation," Macromolecules 22, 1988-1994 (1989).
- 33 J. F. Douglas, J. Dudowicz, and K. F. Freed, "Lattice model of equilibrium polymerization. VI. Measures of fluid 'complexity' and search for generalized corresponding states," J. Chem. Phys. 127, 224901 (2007).
- ³⁴J. Dudowicz, K. F. Freed, and J. F. Douglas, "Lattice model of equilibrium polymerization. IV. Influence of activation, chemical initiation, chain scission and fusion, and chain stiffness on polymerization and phase separation," J. Chem. Phys. 119, 12645-12666 (2003).
- 35 J. Sengers and J. M. H. L. Sengers, "Thermodynamic behavior of fluids near the critical point," Annu. Rev. Phys. Chem. 37, 189-222 (1986).
- 36 B. H. Zimm, "The scattering of light and the radial distribution function of high polymer solutions," J. Chem. Phys. **16**, 1093–1099 (1948). ³⁷H. Benoit, "On the effect of branching and polydispersity on the angular dis-
- tribution of the light scattered by Gaussian coils," J. Polym. Sci. 11, 507-510
- $^{\bf 38}{\rm M.}$ Muthukumar, "Double screening in polyelectrolyte solutions: Limiting laws and crossover formulas," J. Chem. Phys. 105, 5183-5199 (1996).

- ³⁹P.-G. De Gennes, "Critical behaviour for vulcanization processes," J. Phys. Lett. 38, 355-358 (1977).
- ⁴⁰Y. Okada and F. Tanaka, "Cooperative hydration, chain collapse, and flat LCST behavior in aqueous poly(N-isopropylacrylamide) solutions," Macromolecules 38, 4465-4471 (2005).
- ⁴¹M. D. Schwartz, Quantum Field Theory and the Standard Model (Cambridge University Press, 2014).
- ⁴²M. Ishida and F. Tanaka, "Theoretical study of the postgel regime in thermoreversible gelation," Macromolecules 30, 3900–3909 (1997).
- ⁴³M. Doi and S. F. Edwards, *The Theory of Polymer Dynamics* (Oxford University Press, 1988), Vol. 73.
- 44 P.-G. De Gennes, "Qualitative features of polymer demixtion," J. Phys. Lett. 38, 441-443 (1977)
- ⁴⁵J. Joanny, "Critical properties of a system of two molten polymers," J. Phys. A: Math. Gen. 11, L117 (1978).
- ⁴⁶J. Dudowicz, M. Lifschitz, K. F. Freed, and J. F. Douglas, "How far is far from critical point in polymer blends? Lattice cluster theory computations for structured monomer, compressible systems," J. Chem. Phys. 99, 4804-4820 (1993)
- ⁴⁷M. E. Fisher, "Theory of multicritical transitions and the spin-flop bicritical point," AIP Conf. Proc. 24, 273–280 (1975).

 48 R. Kita, T. Dobashi, T. Yamamoto, M. Nakata, and K. Kamide, "Coexistence
- curve of a polydisperse polymer solution near the critical point," Phys. Rev. E 55,
- ⁴⁹P. B. Warren, "Combinatorial entropy and the statistical mechanics of polydispersity," Phys. Rev. Lett. **80**, 1369 (1998). ⁵⁰ M. Kardar, *Statistical Physics of Fields* (Cambridge University Press, 2007).
- 51 K. G. Wilson and J. Kogut, "The renormalization group and the ϵ expansion," Phys. Rep. 12, 75-199 (1974).
- ⁵²M. E. Peskin, An Introduction to Quantum Field Theory (CRC Press,
- ⁵³J. Zinn-Justin, Quantum Field Theory and Critical Phenomena (Oxford University Press, 2002), Vol. 171.
- ⁵⁴M. E. Fisher, "Correlation functions and the critical region of simple fluids," J. Math. Phys. 5, 944-962 (1964).
- ⁵⁵C. A. Tracy and B. M. McCoy, "Examination of the phenomenological scaling functions for critical scattering," Phys. Rev. B 12, 368 (1975).
- ⁵⁶M. E. Fisher, "Renormalization of critical exponents by hidden variables," Phys. Rev. 176, 257 (1968).
- ⁵⁷B. Widom, "Plait points in two- and three-component liquid mixtures," J. Chem. Phys. 46, 3324–3333 (1967).

- ⁵⁸ A. B. Harris, T. C. Lubensky, W. K. Holcomb, and C. Dasgupta, "Renormalization-group approach to percolation problems," Phys. Rev. Lett. 35,
- ⁵⁹M. Borinsky, J. Gracey, M. Kompaniets, and O. Schnetz, "Five-loop renormalization of ϕ^3 theory with applications to the Lee-Yang edge singularity and percolation theory," Phys. Rev. D 103, 116024 (2021).
- $^{\bf 60} J.$ Wang, Z. Zhou, W. Zhang, T. M. Garoni, and Y. Deng, "Bond and site
- percolation in three dimensions," Phys. Rev. E 87, 052107 (2013).

 61 M. Rubinsten and R. H. Colby, Polymer Physics (United States of America, 2003).
- $^{\bf 62}{\rm Y}.$ Ma, S. Ali, and V. M. Prabhu, "Enhanced concentration fluctuations in model polyelectrolyte coacervate mixtures along a salt isopleth phase diagram," Macromolecules 54, 11338-11350 (2021).
- ⁶³H. B. Bohidar and S. S. Jena, "Kinetics of sol-gel transition in thermoreversible gelation of gelatin," J. Chem. Phys. 98, 8970-8977 (1993).
- ⁶⁴V. Prabhu, M. Muthukumar, G. D. Wignall, and Y. B. Melnichenko, "Polyelectrolyte chain dimensions and concentration fluctuations near phase boundaries," J. Chem. Phys. 119, 4085-4098 (2003).
- ⁶⁵ J. L. Sengers, A. H. Harvey, and S. Wiegand, "17 ionic fluids near critical points and at high temperatures," in Experimental Thermodynamics (Elsevier, 2000), Vol. 5, pp. 805-847.
- $^{\bf 66}{\rm A.~Z.}$ Panagiotopoulos and S. K. Kumar, "Large lattice discretization effects on the phase coexistence of ionic fluids," Phys. Rev. Lett. 83, 2981 (1999).
- ⁶⁷K. Rah, K. F. Freed, J. Dudowicz, and J. F. Douglas, "Lattice model of equilibrium polymerization. V. Scattering properties and the width of the critical regime for phase separation," J. Chem. Phys. 124, 144906 (2006).
- ⁶⁸F. Sciortino, E. Bianchi, J. F. Douglas, and P. Tartaglia, "Self-assembly of patchy particles into polymer chains: A parameter-free comparison between wertheim theory and Monte Carlo simulation," J. Chem. Phys. 126, 194903 (2007).
- ⁶⁹ J. Dudowicz, K. F. Freed, and J. F. Douglas, "Flory-Huggins model of equilibrium polymerization and phase separation in the stockmayer fluid," Phys. Rev. Lett. 92, 045502 (2004).
- ⁷⁰K. Van Workum and J. F. Douglas, "Equilibrium polymerization in the stockmayer fluid as a model of supermolecular self-organization," Phys. Rev. E 71, 031502 (2005).
- $^{\bf 71}$ D. J. Audus, F. W. Starr, and J. F. Douglas, "Coupling of isotropic and directional interactions and its effect on phase separation and self-assembly," J. Chem. Phys. 144, 074901 (2016).
- 72D. J. Audus, F. W. Starr, and J. F. Douglas, "Valence, loop formation and universality in self-assembling patchy particles," Soft Matter 14, 1622-1630 (2018).